

This is an Open Access document downloaded from ORCA, Cardiff University's institutional repository: <https://orca.cardiff.ac.uk/id/eprint/136367/>

This is the author's version of a work that was submitted to / accepted for publication.

Citation for final published version:

Varricchio, Carmine , Beirne, Kathy, Aeschlimann, Pascale, Heard, Charles , Rozanowska, Malgorzata , Votruba, Marcela and Brancale, Andrea 2020. Discovery of Novel 2-Aniline-1,4-naphthoquinones as potential new drug treatment for Leber's hereditary optic neuropathy (LHON). *Journal of Medicinal Chemistry* 63 (22) , 13638 -13655. 10.1021/acs.jmedchem.0c00942

Publishers page: <http://dx.doi.org/10.1021/acs.jmedchem.0c00942>

Please note:

Changes made as a result of publishing processes such as copy-editing, formatting and page numbers may not be reflected in this version. For the definitive version of this publication, please refer to the published source. You are advised to consult the publisher's version if you wish to cite this paper.

This version is being made available in accordance with publisher policies. See <http://orca.cf.ac.uk/policies.html> for usage policies. Copyright and moral rights for publications made available in ORCA are retained by the copyright holders.



Title: The discovery of novel 2- aniline- 1,4 naphthoquinones as potential new drug treatment for Leber's hereditary optic neuropathy (LHON)

Carmine Varricchio* ^{a,b}, Kathy Beirne^b, Pascale Aeschlimann^{a,b}, Charles Heard^a, Malgorzata Rozanowska^b, Marcela Votruba^{b,c}, Andrea Brancale^a

^a School of Pharmacy and Pharmaceutical Sciences, Cardiff University, CF10 3NB, Wales, UK.

^b School of Optometry and Vision Sciences, Cardiff University, CF10 3NB Wales, UK.

^c Cardiff Eye Unit, University Hospital of Wales, Heath Park, Cardiff CF24 4LU, Wales, UK

Abstract: LHON is a rare genetic mitochondrial disease, and the primary cause of chronic visual impairment for at least 1 in 10,000 individuals in the United Kingdom. Treatment options remain limited, with only a few drug candidates and therapeutic approaches, either approved or in development. Recently, idebenone has been investigated as drug therapy in the treatment of LHON, although evidence for the efficacy of idebenone is limited in the literature. NQO1 and mitochondrial complex III were identified as the major enzymes involved in idebenone activity. Based on this mode of action, computer-aided techniques and structure-activity relationship (SAR) optimization studies led to the discovery of a series naphthoquinone-related small molecules, with a comparable ATP rescue activity of idebenone. Among these, three compounds showed activity in the nM range and one, 2-((4- fluoro-3-(trifluoromethyl)phenyl)amino)-3-(methylthio)naphthalene-1,3-dione (**1**), demonstrated significantly higher potency *ex-vivo*, and significantly lower cytotoxicity, than idebenone.

Introduction:

Leber's hereditary optic neuropathy (LHON) is a primary mitochondrial DNA (mtDNA) disorder, responsible for acute bilateral visual loss in young adults with a prevalence of 1 in 30,000.¹ Three primary mitochondrial DNA mutations are involved in the development of the disease. The first mutation identified was found in the gene that codes for NADH dehydrogenase 4 (ND4), which is an essential subunit in the mitochondrial complex I core proteins, required to catalyze NADH dehydrogenation and electron transfer to ubiquinone.² Among all the mutation, the ND4 accounts for about 70% of all LHON cases worldwide. The remaining cases are primarily related to mutation polypeptide subunits of ubiquinone ND1 and ND6, which are apparently involved in attaching the hydrophilic part of the enzyme to the inner membrane.³ All these mutations lead to electron flow

blockade at the first step of the mitochondrial electron transport chain (ETC), with deleterious consequence in the ATP production (Figure 1).

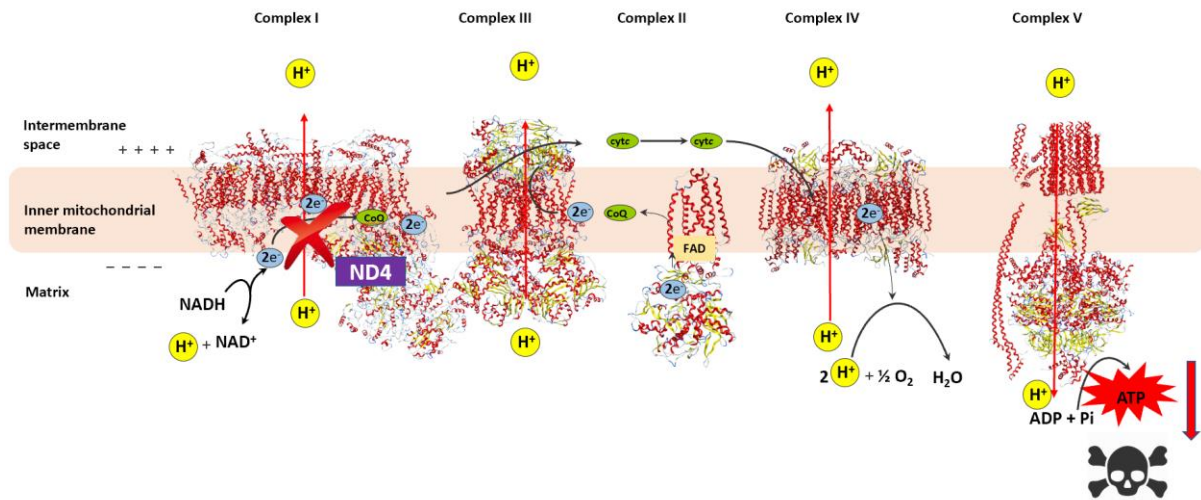


Figure 1 Impairment of mitochondrial electron transport chain (ETC) due to ND4 mutation.

Retinal ganglion cells (RGCs) are particularly susceptible to the decrease of ATP caused by loss of proper mitochondrial activity, which ultimately leads to cellular apoptosis.⁴ RGCs are responsible for the communication between the eye and the brain, taking visual information from photoreceptors and sending to the brain through the optic nerve. The propagation of these signals down their axons demands a large amount of energy, more than other cells, which is mostly the reason for the almost selective visual loss rather than other symptoms (cardiac arrhythmias, peripheral neuropathies, dystonia have occasionally been observed)⁵. To date, a definitive cure is still not available and many of the therapies currently being developed focus on vision management and slowing the progression of the disorder, with a few promising drugs under clinical investigation.^{6,7,8} Most clinical trials are dedicated to either nutritional interventions or redox-active supplements such as idebenone, MTP-131, EPI-743, EPI-589 KL1333 and CoQ10 (Figure 2).⁶

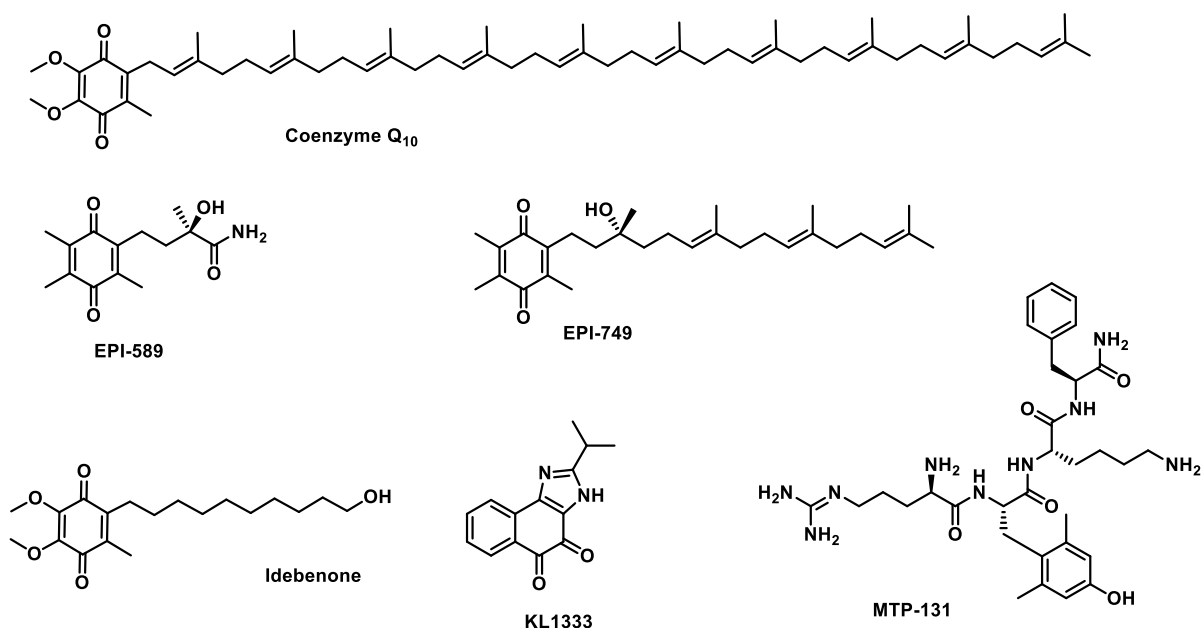


Figure 2 Compounds under clinical investigation

Among them, the idebenone is the only drug to have been approved by the European Medicines Agency as treatment for LHON (in 2015), but only under "exceptional circumstances", with the requirement for continued evaluation of its clinical benefits. Indeed, the evidence for idebenone efficacy is limited, and it failed to demonstrate superiority over placebo in the primary randomized, double-blind, placebo-controlled study.⁹ The beneficial effects associated with idebenone have not been reliably determined in the studies conducted so far, with some patients completely failing to respond to the therapy¹⁰. On the other hand, various papers have reported adverse effects of idebenone, which involve different bodily targets and pathways.^{11,12,13,14}

Although, the mechanism of action of idebenone has not yet been fully elucidated, research has shown evidence that cytosolic NAD(P)H: quinone oxidoreductase 1 (NQO1) is involved in idebenone therapeutic activation; where idebenone is reduced by NQO1 in its active form (idebenol), allowing the transfer of electrons from the cytosol directly to complex III, thus providing an alternative source of electrons for Complex III, thereby restoring the flow of electrons in the ETC (Figure 3).^{15,16} The adverse effects are most likely due to the oxidated form of idebenone, which showed a pro-oxidant effect in NQO1-deficient cells.¹⁷

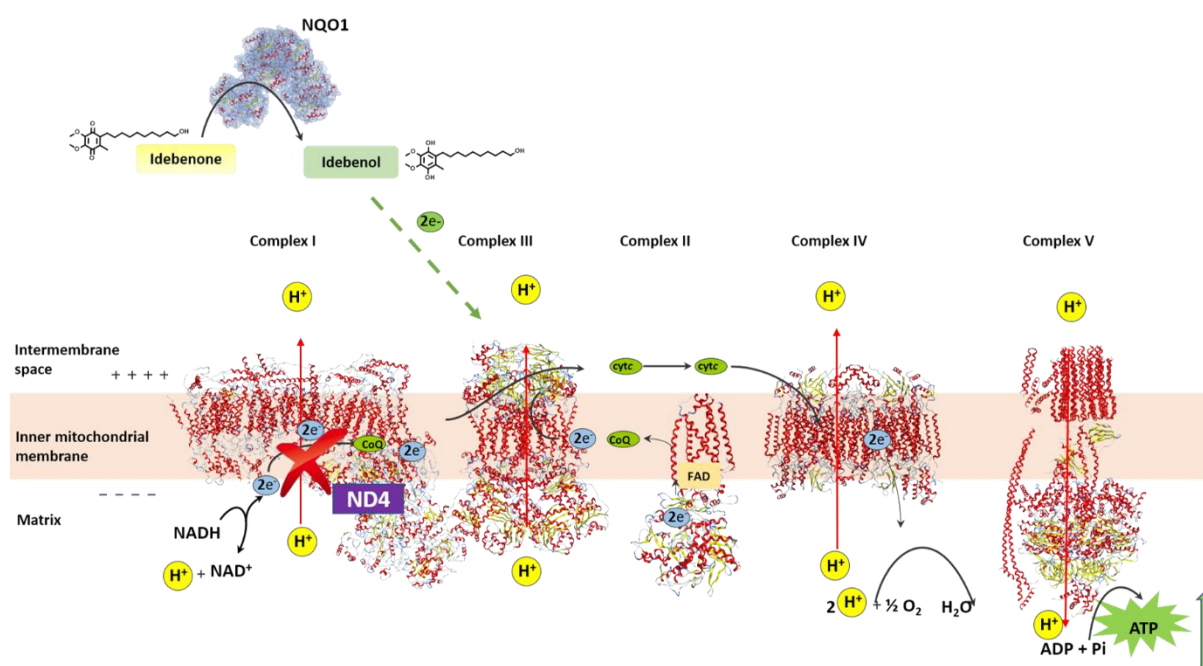


Figure 3 NQO1-Complex III pathway. In the postulated mechanism of action, idebenone is reduced into idebenol (the active form) by NQO1 in the cytoplasm, and then it can successively mediate electron transfer to complex III in the mitochondrial inner membrane, reactivating electron flow.

Due to the aforementioned shortcomings of idebenone and the hypothesis of its mechanism of action, this study aimed to identify new potential drugs which possess a “complex I bypass” capacity, targeting the NQO1-complex III pathway. To achieve this, we performed a sequential ligand- and structure-based virtual screening, resulted in the identification of a hit compound, which was followed by SAR optimization efforts that led to the identification of novel potent redox molecules.

Results and discussion

Virtual screening

From the crystal structures of NQO1 with different substrates ((PDB ID: 2F1O¹⁸, 5EAI¹⁹ and 1H69²⁰, 1D4A²¹) the most important features for ligand binding were identified: an aromatic quinone ring to make a π - π stacking with isoalloxazine of FAD and the presence of two electron acceptors, essential for the redox capacity (Supporting Information Figure S1). These features were used to generate a pharmacophore query and screen a database of more than 3.3 million commercially available compounds (ChemDiv, Specs, Enamine, LifeChemicals). The compounds matching the pharmacophore features were further investigated for their binding mode into the human NQO1 protein using GLIDE SP docking algorithm. These two processes, combined with a visual inspection, led to the identification of 2845 compounds, which show a suitable orientation in the binding site and present the desired redox properties. Not surprisingly, the majority of the identified compounds were quinone-related

molecules: benzoquinones, naphthoquinones, anthraquinones (Figure 4). Next, a second docking study was conducted using the previously selected compounds to evaluate their ability to bind the Qo binding-site of complex III, since these compounds, once they are activated from NQO1, they have to interact with Complex III in order to transfer electrons. The docking studies were performed using a homology-model of human cytochrome bc1 complex (Supporting Information Figure S2). This model revealed that the Qo pocket is highly hydrophobic with six prominent aromatic residues in addition to several aliphatic residues, and most compounds selected could be well accommodated in different rational configurations with the quinone core inside of the cavity and the side-chain close to the opening to the phospholipid membrane (Figure 4). This binding mode is similar to the postulated binding of ubiquinone - the hydroquinone headgroup needs to be close to the 2Fe-2S cluster in order to allow the electrons transfer and the long-chain anchored to the lipid membrane.²² Interestingly, the strong interaction between the phenyl moiety of compound **20** and Phe274 could be essential for the correct positioning of the naphthoquinones into the pocket (Figure 4). To explore the biological activity of these compounds, a final selection of 21 compounds was made based on the affinity for both proteins.

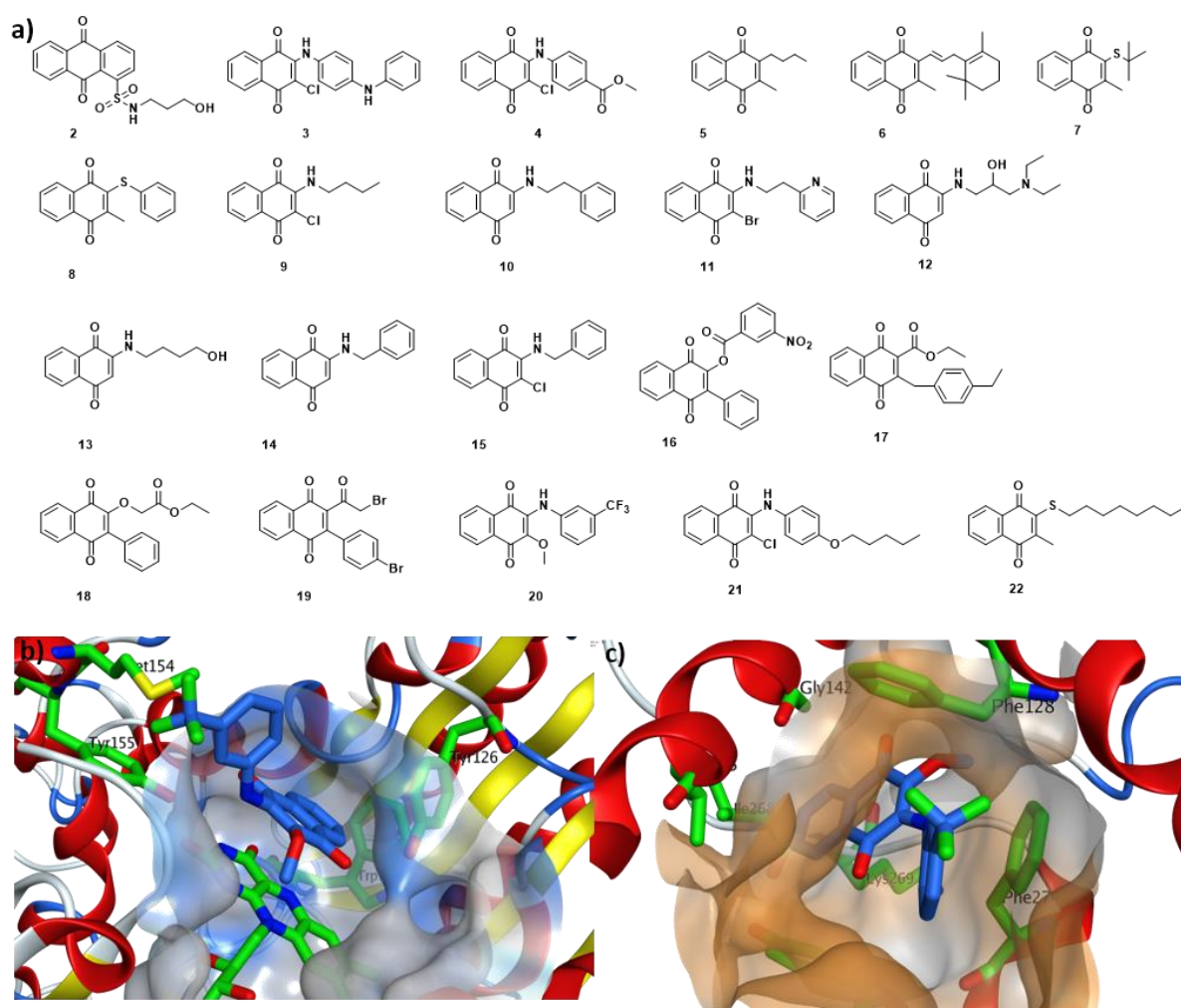


Figure 4. (a) The chemical structures of the final rationally selected commercially available naphthoquinone compounds Predicted binding mode for compound **20** (in blue) in the NQO1-binding site, PDB ID: 2F1O (b) and the complex III-binding site, PDB ID: 1NTZ (c), the amino acid residues involved in the binding are highlighted in green.

Hit identification

In our previous study, we showed the cytotoxicity and ATP rescue activity of idebenone are linked to the cellular expression of NQO1¹⁷: cells deficient in NQO1 show a marked decrease in viability in comparison to NQO1 expressing cells, with idebenone causing ROS production and deleterious effects on ATP levels and cell viability. For this reason, the activity of the 21 selected compounds was tested in two independent cell lines featuring either high (HepG2) or low (SH-SY5H) NQO1 expression since, to date, a valid cell line model to study RGCs is not yet available. The 21 naphthoquinones were initially evaluated for their ability to rescue the ATP level under the inhibition of complex I using rotenone. The treatment of these cells with rotenone (10 μ M) drastically reduced ATP levels to 8% residual ATP

in glucose-free medium. However, the addition of analogs **4**, **7**, **8**, **9**, **15** and **20** almost re-established the same concentration of ATP of idebenone (~70% rescue of ATP, Figure 5a). The most active compounds were re-tested at a lower concentration (1 μ M), showing that quinones with a benzyl ring in position 2 (**15**, **20**) provided a significant ATP rescue activity (Figure 5b).

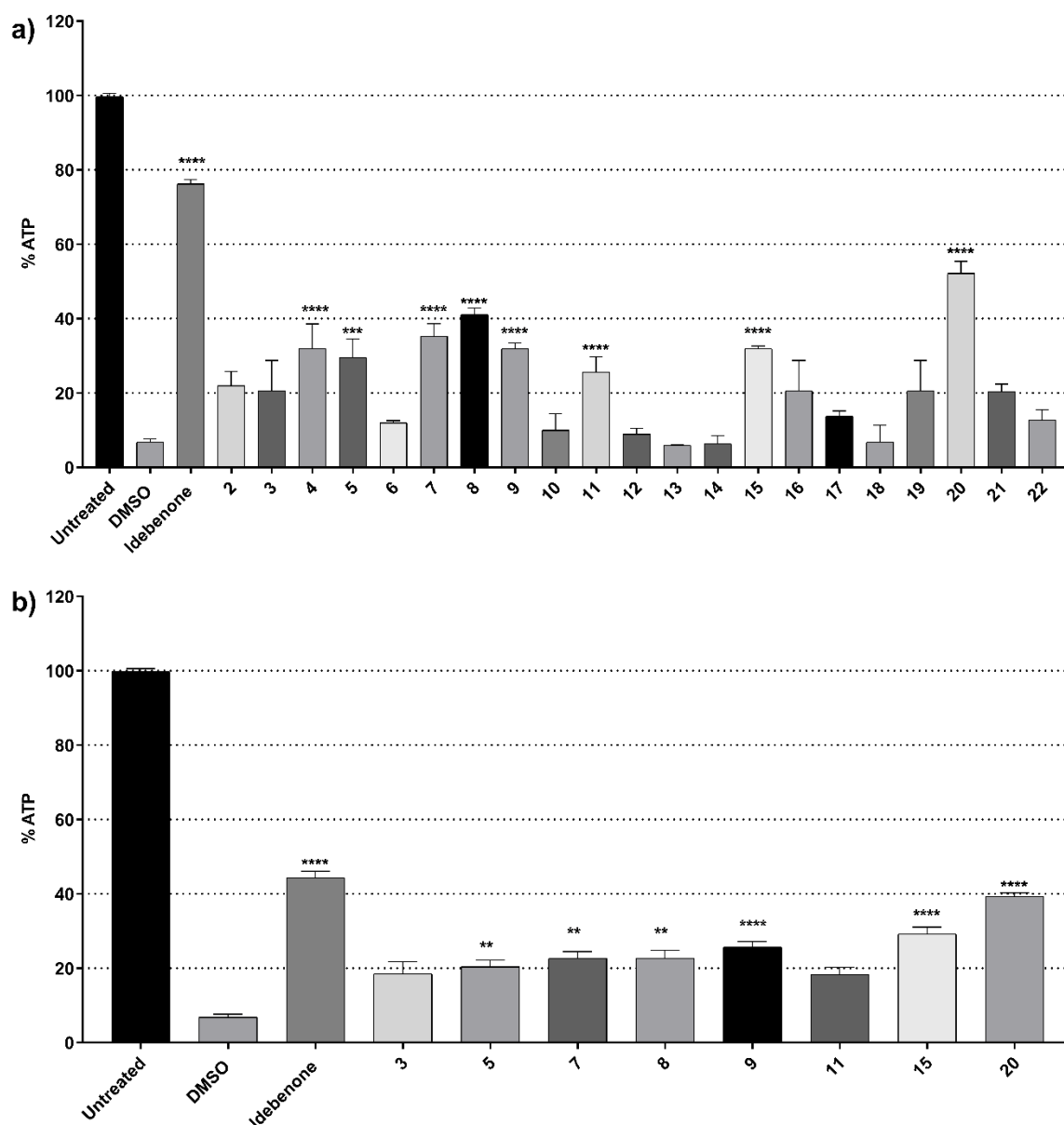


Figure 5 Efficacy of ATP rescue in the presence of 10 μ M rotenone by quinones at 5 μ M (a) and 1 μ M (b). ATP rescue activity of quinones was determined in rotenone-treated HepG2 cells. ATP levels expressed as percentage of ATP in DMSO-treated cells in the absence of rotenone (untreated). Bars represent mean \pm SEM of at least three independent measurements. Data were analysed using one-way ANOVA test, followed by Dunnett's post hoc test for multiple comparisons, *P* values were calculated versus DMSO, * = $p \leq 0.05$, ** = $p \leq 0.01$, *** = $p \leq 0.001$, **** = $p \leq 0.0001$

The compounds that showed significant ATP rescue activity were further tested to determine whether they show a cytotoxic effect using HepG2 and SH-SY5Y cell lines. Naphthoquinone compounds showed a moderately toxic effect at 25 μ M with a decrease of 10-20% of cell viability compared to the untreated cells in HepG2, with the exception of **3** and **4** (Figure 6a), but interestingly the majority of the naphthoquinones showed lower toxicity than idebenone in the SH-SY5Y cell line (Figure 6b). The results suggested that the toxicity of these compounds might be related to the higher affinity of naphthoquinone to NQO1 than to the other oxidoreductases, such as complex I. In fact, idebenone showed deleterious oxidative stress in the NQO1 deficient cell lines, and several studies have reported evidence of this potential adverse effect due to the interaction with other proteins such as complex I²³ or calcium-activated chloride channel¹⁴, inducing oxidative stress and apoptosis in cells.

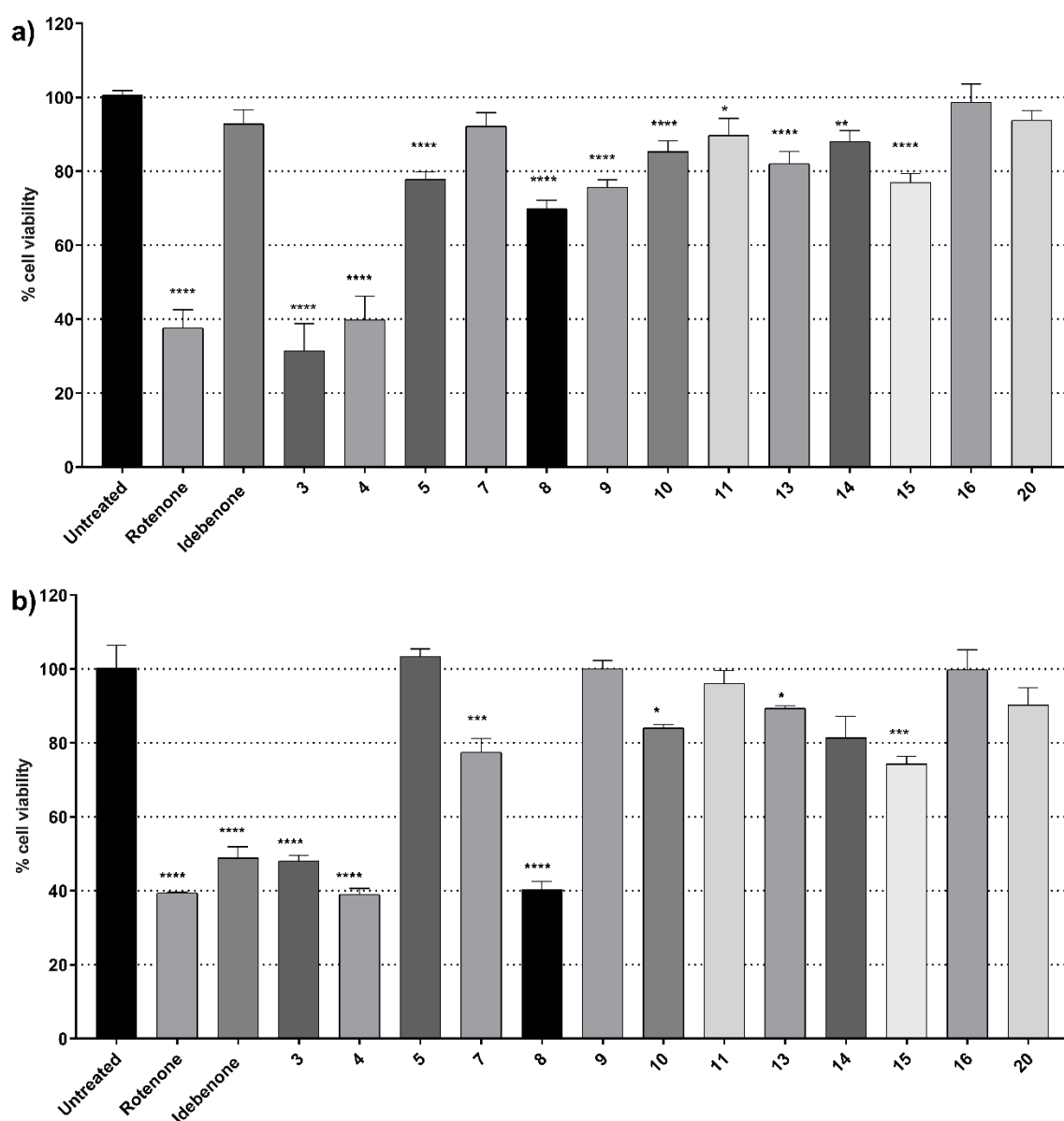
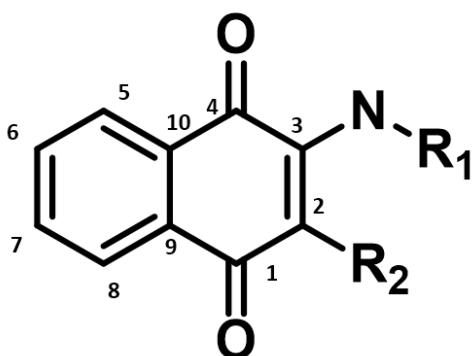


Figure 6 Cytotoxicity of rotenone and quinones (25 μ M) selected from virtual screening on HepG2 (a) and SH-SY5Y(b). The cell viability was determined as percentage of untreated cells. Bars represent mean \pm SEM of at least three independent measurements. Data were analysed using one-way ANOVA test, followed by Dunnett's post hoc test for multiple comparisons, *P* values were calculated versus untreated, * = $p \leq 0.05$, ** = $p \leq 0.01$, *** = $p \leq 0.001$, **** = $p \leq 0.0001$

The analogues **9**, **15** and **20** provided an initial SAR profile since they were sharing the same scaffold: 2- amine 1,4 naphthoquinones. In particular, the compound **20** was pinpointed as the most promising naphthoquinone to study structure-activity relationships, in order to identify compounds with complex I bypass capacity and ATP rescue activity, avoiding the idebenone cytotoxicity in SH-SY5Y cell lines, where NQO1 expression is low. Interestingly, during the course of this project, a recent study conducted by Woolley *et al.* identified a series of amide linked redox-active naphthoquinones, which were able to provide cytoprotection from rotenone-induced toxicity (supporting information Figure S3)²⁴. However, direct evidence for the involvement of NQO1 in the bioactivation of naphthoquinones was not assessed in their study.

Drug Design and Synthesis.

Starting from compound **20**, we have then prepared a series of analogues to explore the structure-activity relationships around the naphthoquinone scaffold. We focused on a panel of 3-amine naphthoquinone analogues with various substituents in position 2 (Table 1), as the docking studies established that there was sufficient space in the binding pocket to tolerate bulkier groups at these positions



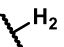
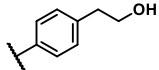
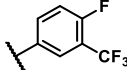
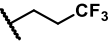
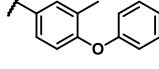
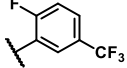
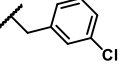
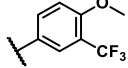
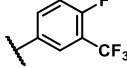
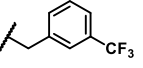
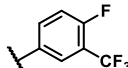
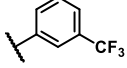
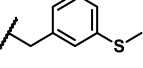
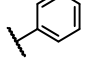
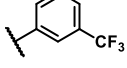
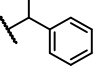
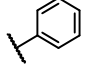
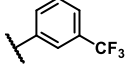
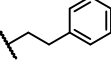
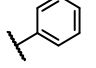
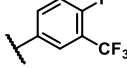
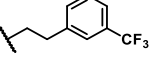
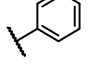
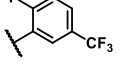
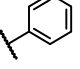
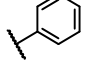
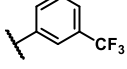
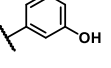
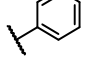
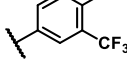
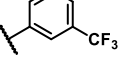
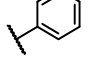
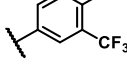
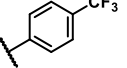
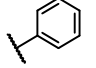
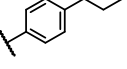
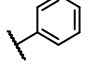
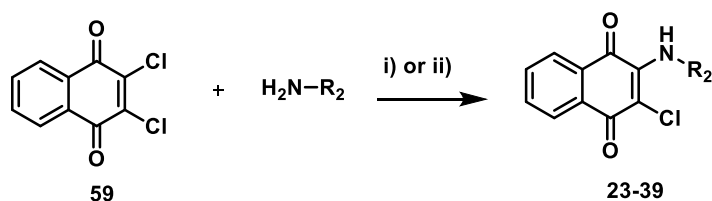
<i>Cpd</i> #	<i>R</i> ₁	<i>R</i> ₂	<i>Cpd</i> #	<i>R</i> ₁	<i>R</i> ₂	<i>Cpd</i> #	<i>R</i> ₁	<i>R</i> ₂
23		Cl	36		Cl	49		OCH ₃
24		Cl	37		Cl	50		OCH ₃
25		Cl	38		Cl	51		NHCH ₃
26		Cl	39		Cl	52		SCH ₃
27		Cl	40		OH	53		SCH ₂ CH ₃
28		Cl	41		OCH ₃	54		SCH(CH ₃) ₂
29		Cl	42		OCH ₂ CH ₃	1		SCH ₃
30		Cl	43		OCH ₂ CH ₂ CH ₃	55		SCH ₃
31		Cl	44		OCH(CH ₃) ₂	56		SCF ₃
32		Cl	45		OC ₆ H ₅	57		SCF ₃
33		Cl	46		NHCH ₃	58		CH ₃
34		Cl	47		NHCH ₂ CH ₃			
35		Cl	48		N(CH ₃) ₂			

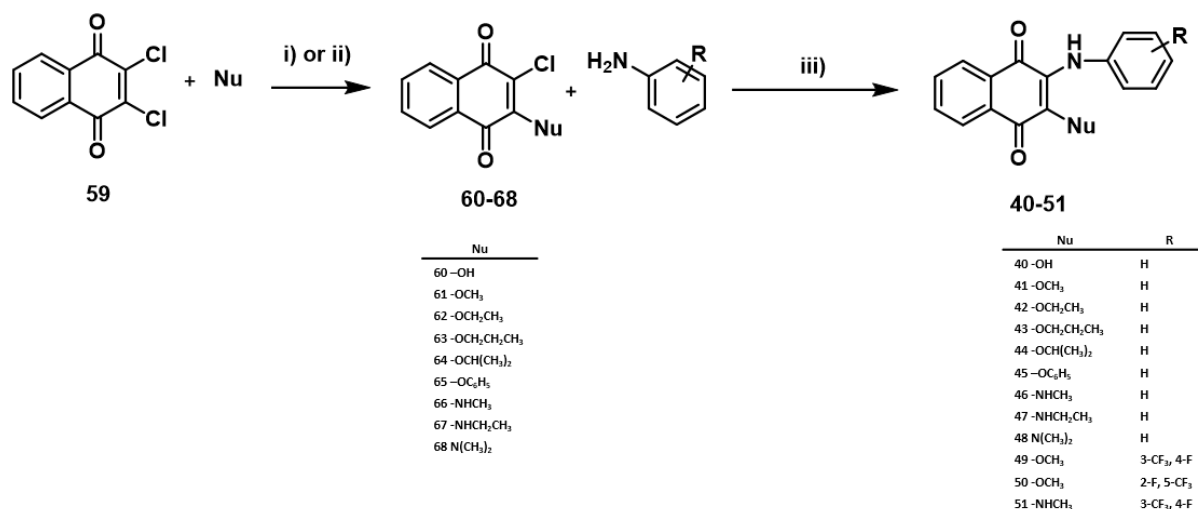
Table 1 General strategy for identifying 37 analogues of compound **20**, showing the chemical structure details of synthesized compounds **1** and **23-58**.

A series of -amine naphthoquinone analogues **23-39** were synthesized via a nucleophilic substitution reaction, treating 2,3-dichloro-1,4-naphthoquinone (**59**) with an excess of the corresponding amine, in ethanol. In the case of low nucleophilic aniline such the 4-fluoro-3-(trifluoromethyl) aniline, CeCl₃ was used as catalyst to facilitate the nucleophilic addition (Scheme 1).



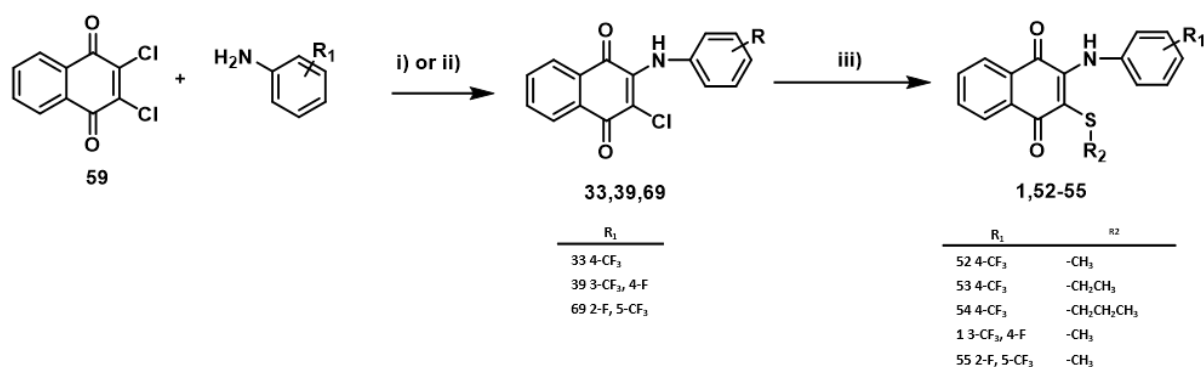
Scheme 1 (i) corresponding amine, EtOH, rt. (ii) 4-fluoro-3-(trifluoromethyl) aniline, $\text{CeCl}_3 \cdot 7\text{H}_2\text{O}$ EtOH, reflux.

After the first substitution and formation of the 2-amino-3-chloro-1,4-naphthoquinone derivative, the reactivity of naphthoquinone core was reduced, due to the increase of electronic density in the ring - the second substitution can occur only in the presence of strongly nucleophilic molecules, such as thiolate or if an EWG group effect is incorporated in the quinone ring. Therefore, a microwave-assisted Buchwald–Hartwig amination strategy was used to replace the second chlorine atom with a series of substituted anilines (Scheme 2).



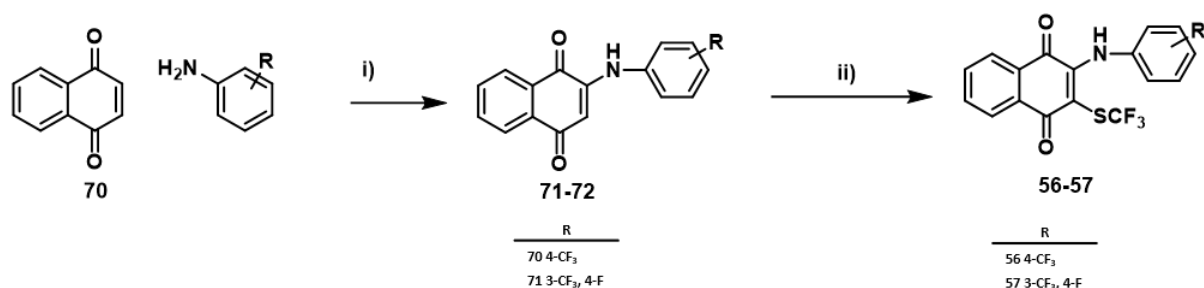
Scheme 2 (i) corresponding alcohol, K_2CO_3 , THF, rt; (ii) corresponding amine, EtOH, rt., (iii) $\text{Pd}_2(\text{dba})_3$, t-BuOK, XPhos, Toulene, mw 130 °C, 30 min

The analogues **1**, **52-55** which have a thiomethoxy in position **2**, was instead synthesized through two sequential nucleophilic substitutions due to the better nucleophilic reactivity of thiolate compared to alkoxide or amine (Scheme 3)



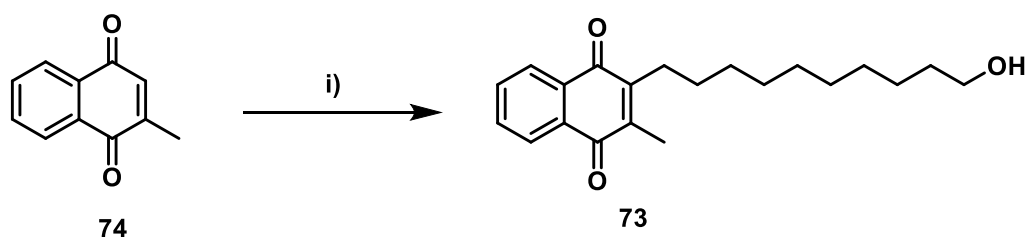
Scheme 3 (i) 3-(trifluoromethyl) aniline, EtOH, rt. (ii) fluoro-3-(trifluoromethyl) aniline, $\text{CeCl}_3 \cdot 7\text{H}_2\text{O}$ EtOH, reflux, ., (iii) corresponding thiol, K_2CO_3 , EtOH

The trifluoromethylthiol derivatives (**56-57**) were synthesized via a radical pathway starting by the intermediate **71-72**, and AgSCF_3 .²⁵ The postulated reaction mechanism involves the SCF_3 radical, formed *in situ* through the oxidation of AgSCF_3 by $\text{K}_2\text{S}_2\text{O}_8$ (Scheme 4)



Scheme 4 (i) corresponding aniline, $\text{CeCl}_3 \cdot 7\text{H}_2\text{O}$ EtOH, reflux (ii) $\text{Cu}_2(\text{OH})_2\text{SO}_3 \cdot \text{H}_2\text{O}$, $\text{K}_2\text{S}_2\text{O}_8$, AgSCF_3 , MeCN 65 °C, 12h

Finally, compound **73** was designed and synthesized as an analogue of idebenone, only replacing the quinone with a naphthoquinone and maintaining the same side-chain. The synthesis of **73** requires a single-step reaction through the Minisci reaction. The installation of an alkyl side chain at the 3-position of the naphthoquinone core was facilitated via a silver-mediated radical decarboxylation (Scheme 5).



Scheme 5 (i) 11-hydroxyundecanoic acid, AgNO_3 , $(\text{NH})_4\text{S}_2\text{O}_8$, MeCN, water, 75 °C, 2h

Biological activity in vitro: ATP rescue and cytotoxicity

Based on the compounds prepared around the naphthoquinone group, the SAR study can be divided into 2 subgroups: structural modifications at C3 to investigate the importance and influence of the aromatic ring, and structural modifications at C2 to study of the effect of EDG and EWG substitutes on the naphthoquinone ring.

Firstly, to determine the minimum structural requirement of the 2-amino-1,4-naphthoquinone scaffold, the phenyl ring at position 2, was removed (**23**), and several analogues were synthesized modifying the length of the linker between the benzoquinone core and phenyl ring (**28,29,31**). The results obtained showed the importance of a phenyl moiety (Figure 7): the removal of the benzyl ring completely eliminated ATP rescue activity (**23**), while replacement with an alkyl chain decreased the potency (**24**). Interestingly, the length of the linker between the benzoquinone core influenced the activity, showing a slight decrease from aniline (**33**) to benzylamine (**26**).

The importance of the trifluoromethylene substituent on the phenyl ring was also investigated, and the corresponding analogues carrying the CF_3 moiety in position 3 of the phenyl ring were synthesized and tested (**14-26, 29-30, 31-33**), showing overall a higher ATP rescue than the no substituted analogues. The replacement of the core from benzoquinone of idebenone to naphthoquinone (**73**) drastically reduced activity, suggesting a totally different structure-activity relationship of this family from the benzoquinone drugs.

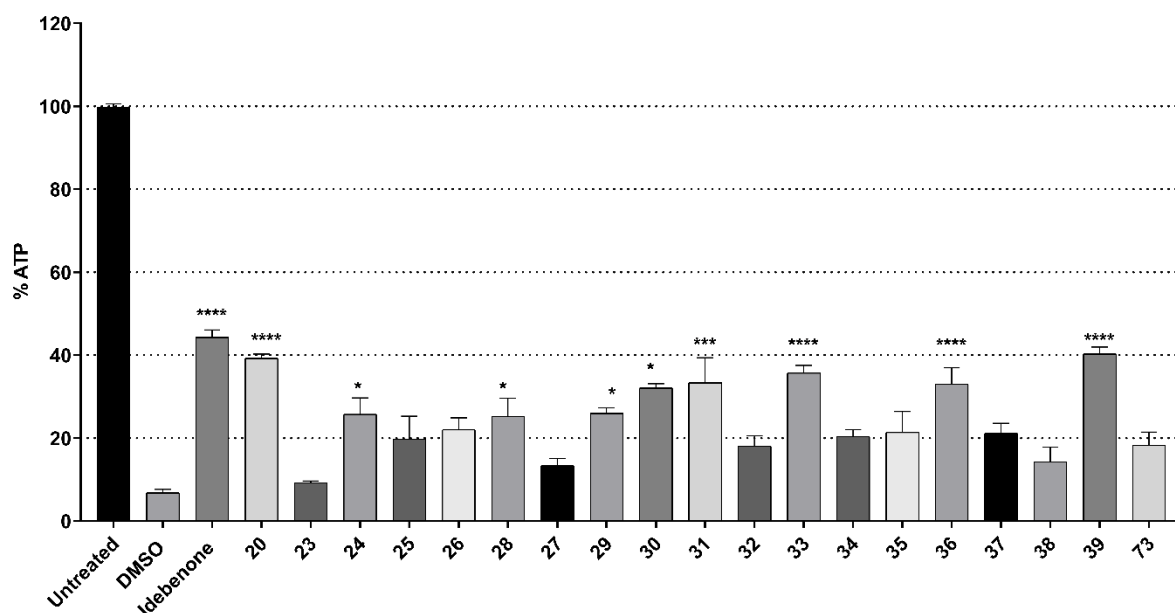


Figure 7 Efficacy of ATP rescue in the presence of rotenone by quinones (23-39, 73) at 1 μ M. ATP levels expressed as percentage of ATP in DMSO-treated cells in the absence of rotenone (untreated). Bars represent mean \pm SEM of at least three independent measurements. Data were analyzed using one-way ANOVA test, followed by Dunnett's post hoc test for multiple comparisons, *P* values were calculated versus DMSO. * = $p \leq 0.05$, ** = $p \leq 0.01$, *** = $p \leq 0.001$, **** = $p \leq 0.0001$

None of the synthesized quinones shows an improved ATP rescue compared to **20**. Moreover, this series of compounds showed higher cytotoxicity than the hit. In particular **33**, which differs by the presence of chlorine instead of OCH_3 in position 2, showed an increase of cytotoxicity, making the methoxy group a better substituent than chlorine (Figure 8). Therefore, nine compounds (**40-48**) were synthesized in order to investigate the effect of the substituent at position 2.

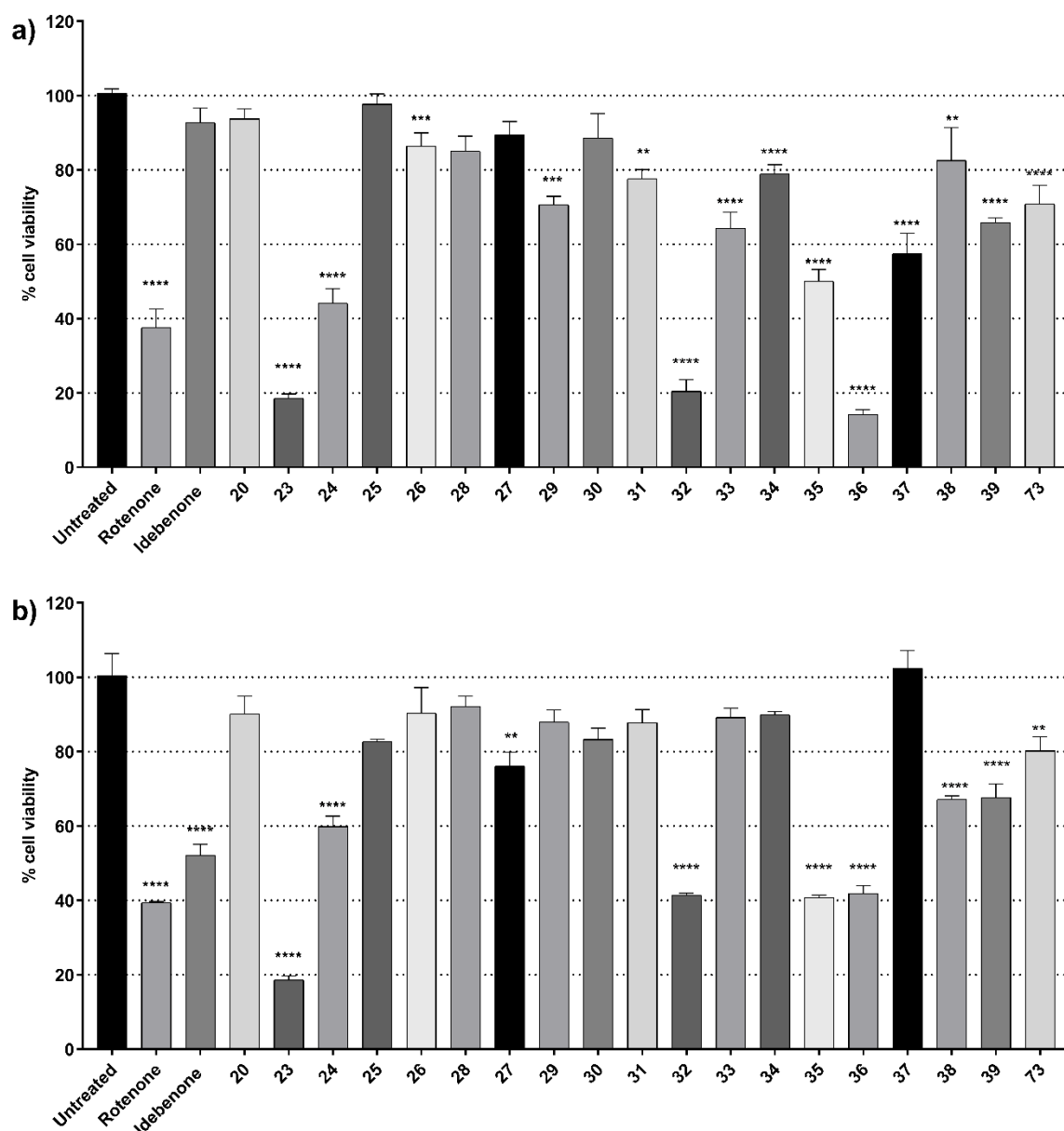


Figure 8 Cytotoxicity of quinones 23-39,73 on HepG2 (a) and SH-5YSY (b) cells at 25 µM. Cell viability was determined as percentage of untreated cells. Bars represent mean \pm SEM of at least three independent measurements. Data were analysed using one-way ANOVA test, followed by Dunnett's post hoc test for multiple comparisons, *P* values were calculated versus untreated, * = $p \leq 0.05$, ** = $p \leq 0.01$, *** = $p \leq 0.001$, **** = $p \leq 0.0001$

The replacement of methyl ether with ethyl ether (**41**) or n-propyl ether (**42**) did not improve the ATP rescue, on the contrary, isopropyl ether **44** and phenyl ether **45** decreased the activity showing that sterically hindering groups are not beneficial. Also, the removal of the ether (**40**) drastically reduced the activity. The effect of bioisostere replacement of the methoxy group with the methylamine decreased the potency (**46**). This trend was observed for the other analogues synthesized, where **47**

and **48** showed lower ATP rescue than the corresponding ether and ester derivatives **41** and **42** (Figure 9). The explanation of this drastic difference suggested that the different reduction potential of these compounds played a key role in the activity of this family. In fact, the presence of a strong electron donating group (EDG) in the ring changes significantly the electron density of compounds, influencing the redox capacity of this family of compounds and decreasing the reduction rate.

In order to study the influence of EDG/EWG groups on the ATP rescue, we investigated the introduction of a more EWG group, replacing the OCH₃ group with an SCF₃ group in position 2 of the naphthoquinone core. Interestingly, **56** and **57** retained the activity, but on the other hand, they also demonstrated an increase of cytotoxicity in both cell lines. For this reason, the methoxy group was instead replaced with a group possessing a similar EDG effect, such as thiomethyl. Compound **1** showed overall a retain of activity, but a slight increase of cytotoxicity compared the ether analogue **20**. The same trend was also observed for the thioethyl and thiopropyl (**53-54**), which showed the same activity than their corresponding ether derivatives. Having demonstrated the importance of the electronic effect of the substituent in the naphthoquinone core, another EDG group with a similar effect of OCH₃ was considered, synthesizing the corresponding methyl derivatives (**58**). Also, in this case, the compounds showed a similar ATP rescue activity and low cytotoxic effect on both cell lines (Figure 9).

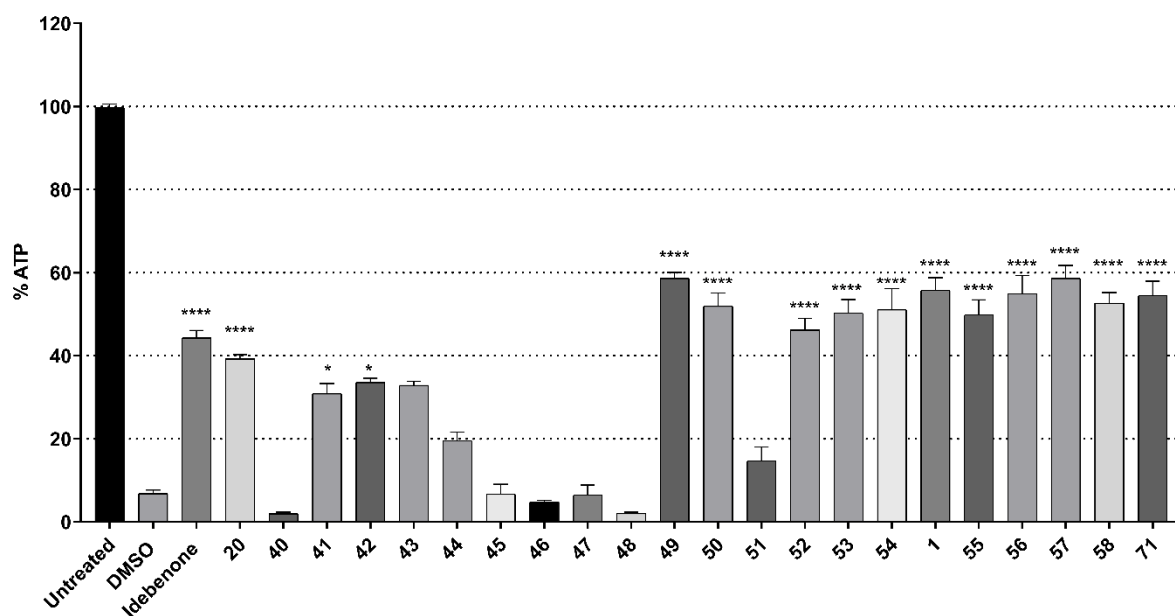


Figure 9 Efficacy of ATP rescue in the presence of rotenone by quinones (**1,40-58,71**) at 1 μ M. ATP levels expressed as percentage of ATP in DMSO-treated cells in the absence of rotenone (untreated). Bars represent mean \pm SEM of at least three independent measurements. Data were analyzed using one-way ANOVA test,

followed by Dunnett's post hoc test for multiple comparisons, *P* values were calculated versus DMSO. * = $p \leq 0.05$, ** = $p \leq 0.01$, *** = $p \leq 0.001$, **** = $p \leq 0.0001$

In summary, we can observe that molecules retaining the aniline group in position 3 showed slightly better activity than benzylamine and phenylethylamine analogues. A complete loss of activity was observed when a strong electron-donating group was introduced in position 2; on the other hand, the presence of strong electron-withdrawing groups increased the cytotoxicity of these family. The presence of a hindering group in position 2 decreased activity, while replacement of methoxy group **49** with a thiomethyl (**1**) or methyl group (**58**) did not alter the activity. Overall, the introduction of fluorine on trifluoromethyl-aniline ring was associated with an increase in the activity (**1,49,50,55,58**). From the cytotoxicity data evaluated on SH-SY5Y the naphthoquinone core providing significantly less toxicity than idebenone. On the other hand, a decrease of 10-25% of viability on HepG2 was shown by the majority of naphthoquinones (Figure 10). In our previous study, we demonstrated that the ratio between reduced/oxidized form of quinones could trigger the beneficial or either the toxic effect of the redox-active compounds¹⁷. In order to clarify the cytotoxicity effect of this family, the naphthoquinones were tested for their capacity to generate ROS in the cells, showing that the most toxic compounds were able to increase drastically the level of H₂O₂ in the cells (Supporting information Figure S4)

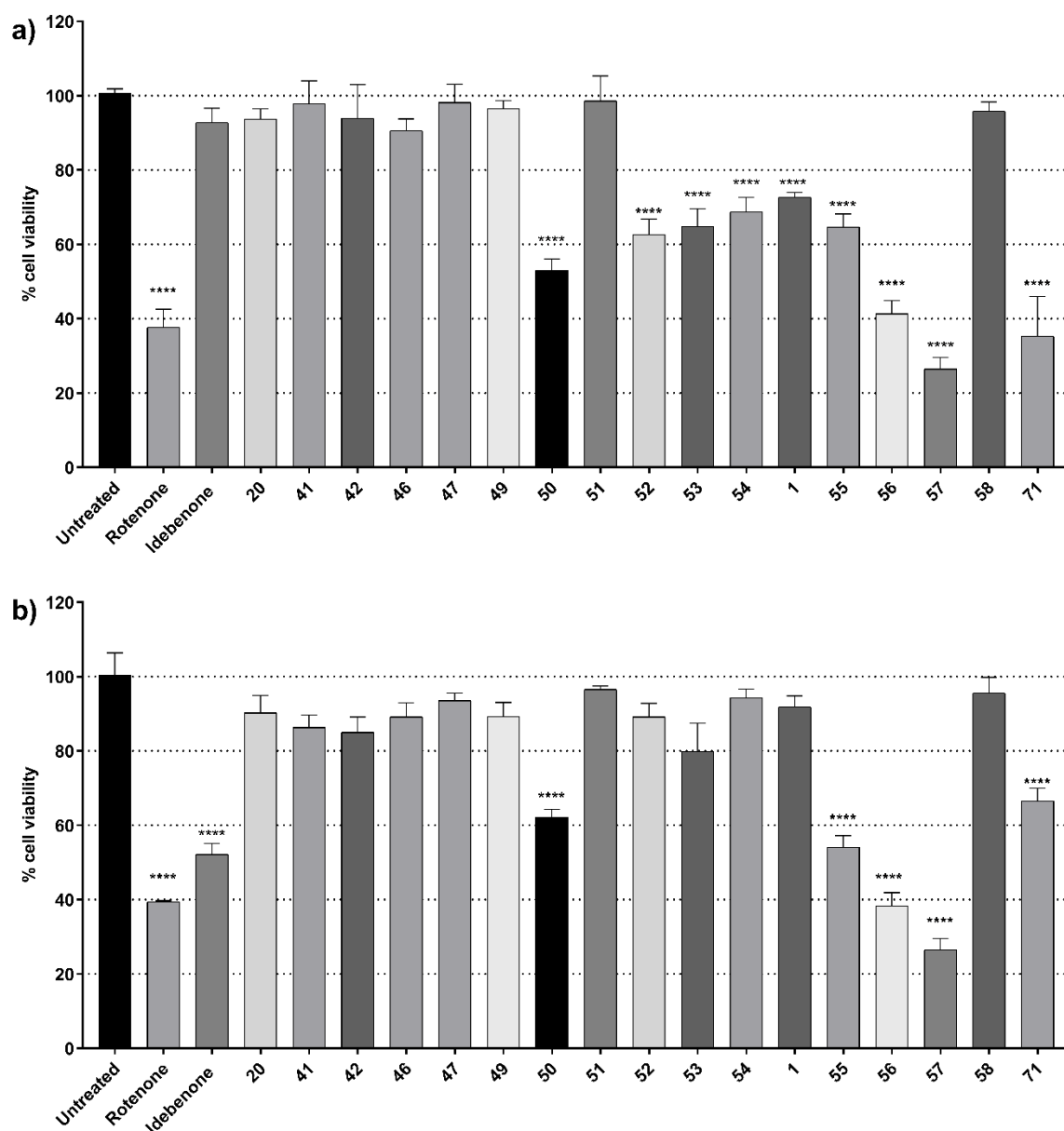


Figure 10 Cytotoxicity of quinones 1,40-58 on HepG2 (a) and SH-5YSY (b) at 25 μ M. The cell viability was determined as percentage of untreated cells. Bars represent mean \pm SEM of at least three independent measurements. Data were analysed using one-way ANOVA test, followed by Dunnett's post hoc test for multiple comparisons, P values were calculated versus untreated, * = $p \leq 0.05$, ** = $p \leq 0.01$, *** = $p \leq 0.001$, **** = $p \leq 0.0001$

Mode of action: NQO1-complex III pathway

Having demonstrated the ATP rescue capacity of these novel identified naphthoquinones, it was of interest to elucidate the postulated mode of action of this family. From the computational studies, naphthoquinone compounds have been identified as an interesting class of organic compounds, which

might easily bind NQO1, accepting two electrons and consequently reducing in hydroquinones. In order to confirm NQO1 affinity, the compounds were tested to determine whether they can be substrates of the NQO1 using the recombinant enzyme. The reduction of quinone into hydroquinone can be followed by the decrease of NADH absorbance at 340 nm, according to the following reaction:



The results obtained suggest that even if naphthoquinones are excellent NQO1 substrates, not all the quinones were reduced by the enzyme in a cell-free environment, in particular, the two 2-amino-1,4-naphthoquinones (**46**, **51**), which show an amine group in position 3, are inactive, confirming the NQO1-dependent ATP rescue of this family (Supporting information Figure S5). Interestingly the amide linked naphthoquinones previously published by Woolley *et al* (supporting information Figure S3 compound **75**), showed a significantly lower affinity for NQO1 than the aniline linked naphthoquinones (**1**, **49**, **51**, **57**), a possible explanation may be found in the different side-chain, which might modulate the affinity for other oxidoreductases as suggested by Woolley *et al.*²⁴. The high NQO1 affinity showed by the aniline-linked naphthoquinones did not exclude a possible reduction of these compounds from other oxidoreductases present in the cells. For this reason, the reduction rate of quinone by NQO1 was assessed in living cells by hydroquinones-mediate WST-1 reduction, as previously reported in literature²⁶. The results showed that the naphthoquinones were highly reduced in HepG2, but only if NQO1 is available. In fact, when the compounds were tested in the presence or not of dicoumarol (NQO1 inhibitor)²¹ and in NQO1-deficient cell line (SH-SY5Y), WST-1 was not converted into its formazan structure due to the lack of electron mediator (hydroquinone), demonstrating the high affinity and high selectivity of these compounds to NQO1. (Figure 11). The assay was repeated in another NQO1-deficient cell line¹⁷, R28 (retinal precursor cell line), where no substantial conversion of WST-1 to formazan was detected (supporting information Figure S6).

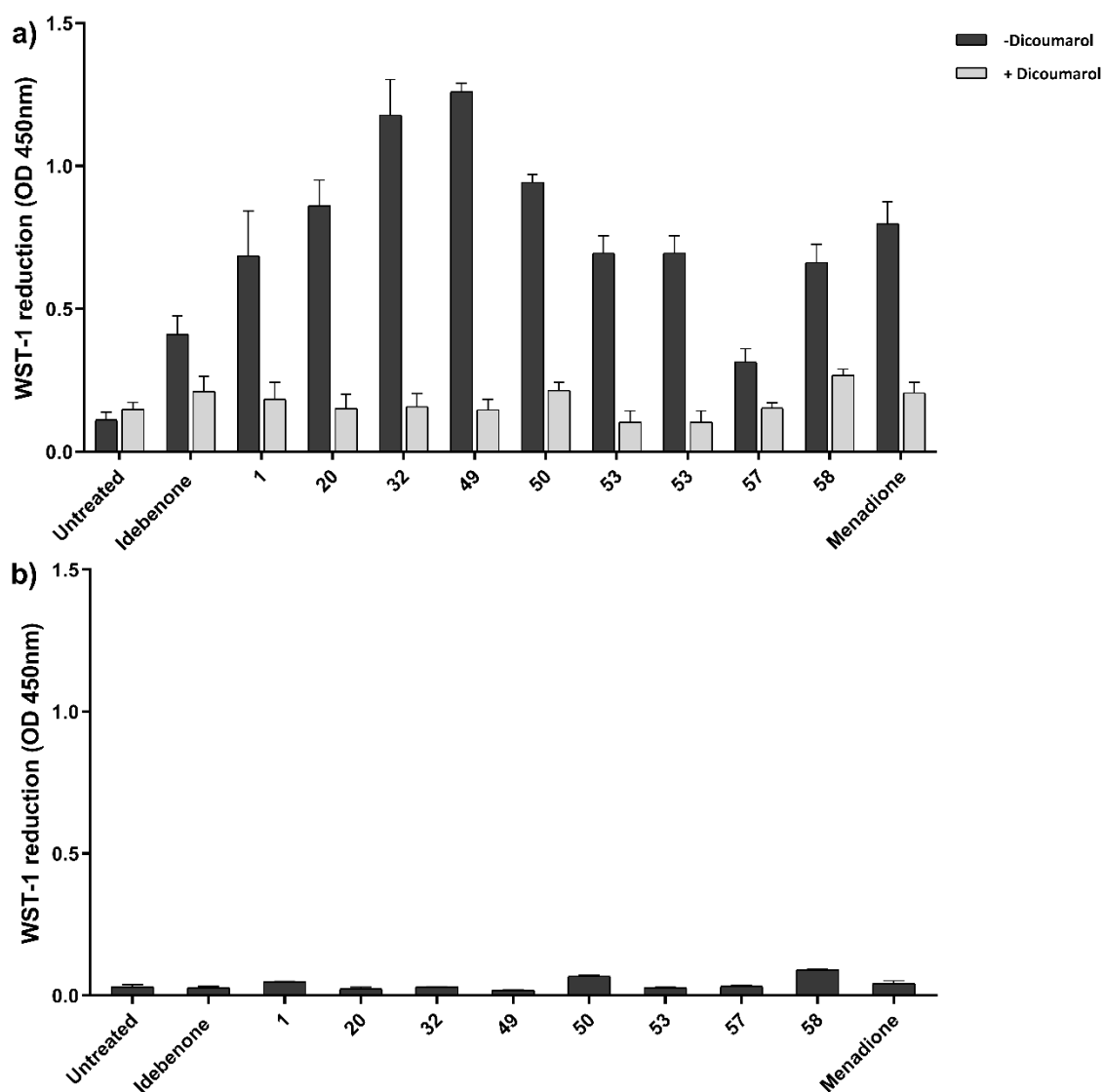


Figure 11 (a) WST-1 reduction in the presence of hydroquinone as electron donor in HepG2 cell line in the absence (black bars) or presence of dicoumarol (grey bars). (b) WST-1 reduction in the presence of hydroquinone as electron donor in HepG2 in NQO1-deficient cell line (SH-SY5Y). The different WST-1 reduction rates depend on different affinities of compounds towards the enzyme: compounds showing a higher affinity for NQO1 could reduce the WST-1 faster than others

These data suggested that these compounds are acting as NQO1 cytosolic-mitochondrial electron carriers, rescuing the ATP level under inhibition of complex I through the NQO1-complex III pathways. If the ATP rescue –activity depends on these enzymes, it should be sensitive to inhibition of complex III and NQO1. Therefore, two NQO1 inhibitors, dicoumarol and ES936, were used to assess the direct involvement of NQO1 in the naphthoquinones bioactivation²⁷. Dicoumarol is a non specific competitive inhibitor that has been frequently used to study the involvement of NQO1 in biochemical

reactions²⁷; meanwhile, ES936 is a potent and specific irreversible NQO1 inhibitor²⁷. The ATP rescue activity of naphthoquinones was lost in both cases, confirming the critical role of NQO1 in the bioactivation of these family (Figure 12). In addition, to confirm the role of complex III, as the terminal electron acceptor, myxothiazol and antimycin were used as inhibitors²⁸. Myxothiazol and antimycin are two selective complex III inhibitors, which bind two different binding sites Q_o, quinol oxidation site, and Q_i, quinol reduction site, respectively. Although these inhibitors influenced the ATP level in untreated cells, even at low concentration (50 nM), the ATP rescue of compounds was lost in all the cases, confirming the direct involvement of Complex III in the naphthoquinone's activity (Figure 12)

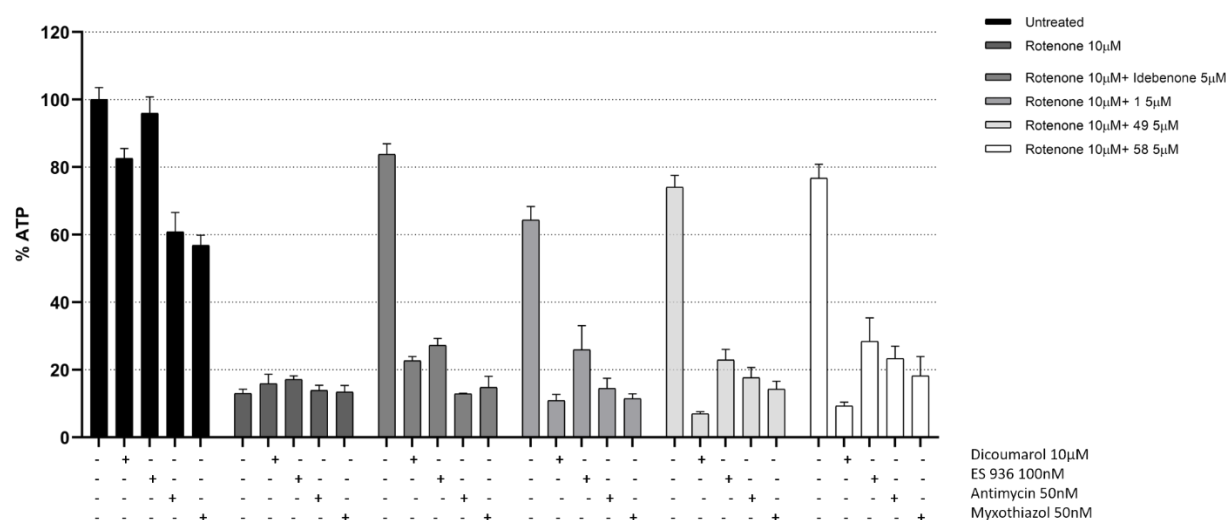


Figure 12 The effect of dicoumarol, ES936, antimycin, myxothiazol on the ATP rescue activity of compounds **1**, **49-58** and idebenone. The ATP rescue activity of compounds (5 µM) were assessed in the presence of rotenone (10 µM) and in the absence (-) or presence of inhibitors (+). ATP levels expressed as percentage of DMSO-treated cells in the absence of rotenone (untreated).

Standard reduction potential r prediction

A difference in the binding mode cannot justify, on its own, the significant difference in the activity and cytotoxicity between **49** and the corresponding analogues **51** and **57**, as the NQO1 possesses a highly plastic active site, which can accommodate quinone compounds of different sizes. A possible explanation might be found in the different reduction potential of these compounds. In fact, while the replacement of methoxy or thiomethyl group to methylamine causes minimal steric perturbations, the effect in the electron density distribution is significant. Recent studies provide strong evidence of a correlation between the energies of HOMO (highest occupied molecular orbital) and LUMO (lowest unoccupied molecular orbital) for the reduced and oxidized forms of studied quinones and the

electrode potentials (Figure 13).^{29,30,31} In order to predict the reduction potential of naphthoquinones, The quinone compound structures were optimized using B3LYP with 6-311+G- (d, p) basis set and the effect of solvation of water was applied using a polarized continuum model (PCM) in the optimization calculation. This procedure was used to evaluate the effect of the reduction potential of the new analogs in their activity, with the possibility to identify a correlation between these two values.

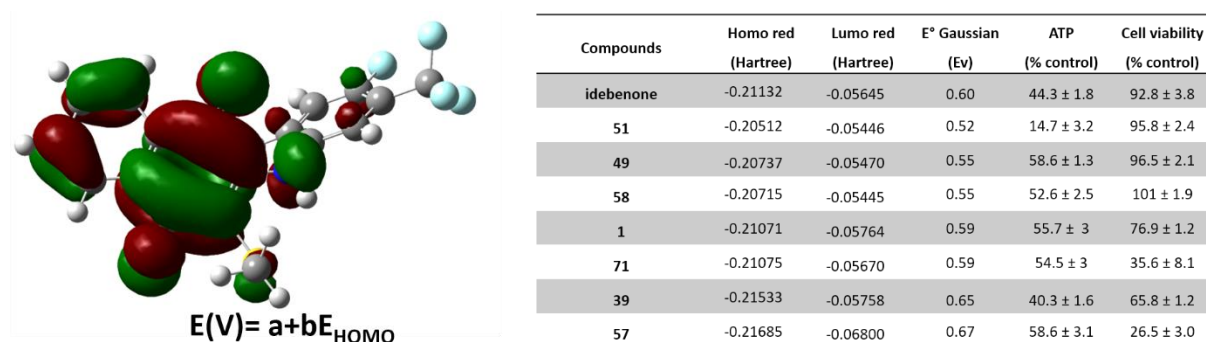


Figure 13 Representations of menadione orbitals elaborated with Gaussian 09. Graphical representation of orbitals of **1** and the equation, which describes the correlation between electrode potential and energy associated with HOMO orbitals, the constants a and b in the equations are -2.115 and -12.845, respectively.

Table 2 Standard reduction potential of naphthoquinones with different EDG/EWG substituents at position 2 with the corresponding ATP rescue and cell viability values

The results, reported in Table 2, shows two distinct trends for the effect of nature and position of the substituents studied on the quinone core., Quinone compounds with electron-donating groups (**1**, **49**, **51**, **58**) show a lower reduction potential in comparison with unsubstituted quinone compounds. The addition of another EDG group in the quinone core might drastically reduce the ability to accept electrons, and therefore they could not be metabolised into hydroquinones by NQO1. As expected, electron-withdrawing groups (**39**, **56**) have an opposite effect, increasing the reduction potential, and consequently facilitate the compound reduction. These results are reasonable because the introduction of substituents leads to a change in the charge distribution in the quinone structure, and therefore it influences the reduction potential: electron-withdrawing substituents facilitate reduction stabilizing the negative charge, whereas electron-donating substituents destabilize it (Figure 14). These results suggest that the reduction potential of quinone compounds can be modulated by the presence of substituents in the aromatic ring, affecting the stability/toxicity of quinones/semiquinones/hydroquinones .

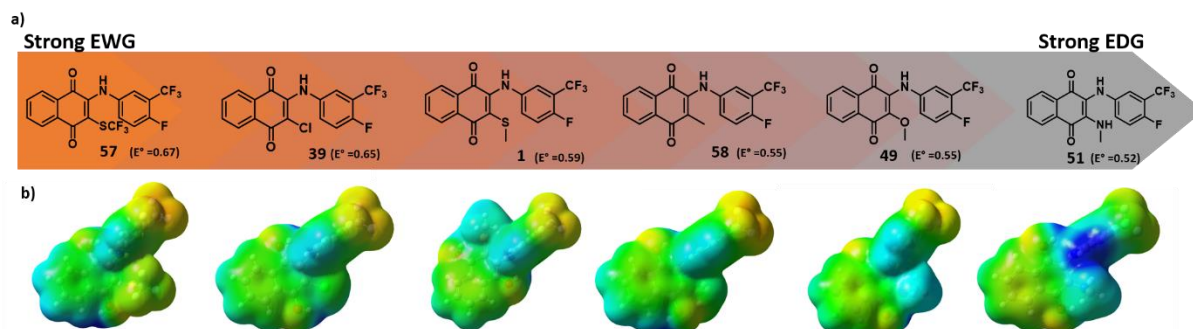


Figure 14 (a) Decrease of standard reduction potential in relation to the electrostatic effect of substituted in position 2. (b) the molecular electrostatic potential map of each molecule.

According to the results obtained, we hypothesize that a naphthoquinone with high standard electron potential as **57** might “steal” electrons from biological redox centers, such as cytochromes, iron-sulfur clusters, and cupredoxins, inhibiting metabolic output. However, **51**, which possesses a low standard electron potential, is not able to accept electrons and therefore remains inactive. Mild redox naphthoquinones, such as **1**, **49** and **58**, might instead be able to generate a useful cycle between oxidized and reduced forms using specific physiologic redox centers, showing a beneficial pharmacological effect (supporting information Figure S7).

Dose-response curve ATP rescue and cytotoxicity

A series of concentration-response studies for the best three compounds (**1,49,58**) and one of the most potent naphthoquinones reported in Woolley’s study (supporting information Figure S3 compound **75**) were performed to determine the half-maximal ATP rescue concentration (EC_{50}) and the half-maximal cytotoxic concentration (IC_{50}) using 6 data points (supporting information Figure S8). The calculation was performed on two different cell lines: HepG2 and SH-SY5Y, which express different levels of NQO1.

Compounds	EC ₅₀	IC ₅₀	IC ₅₀
	(μ M)	HepG2 (μ M)	SH-SY5Y (μ M)
idebenone	0.94 \pm 0.06	64.5 \pm 15.1	15.9 \pm 0.09
1	0.36 \pm 0.05	30.5 \pm 5.2	>100
49	0.46 \pm 0.05	>100	>100
58	0.91 \pm 0.06	>100	>100
S1 75	0.80 \pm 0.03	>100	76.05 \pm 9.1

Table 3. IC₅₀ and EC₅₀ values for idebenone, **1**, **49**, **58** and **75** (figure S3). The EC₅₀ is defined as the concentration of compounds that induce a half-maximal rescue of ATP concentration in rotenone-treated cells. The IC₅₀ is defined as the concentration of compounds that reduce the cell viability by half.

Interestingly, the naphthoquinones **1**, **49** and **58** showed higher activity than idebenone at lower concentration 100 nM - 1 μ M, but they reached a plateau-phase early, without entirely rescuing the ATP level. Meanwhile, idebenone and **75** (figure S3) were almost able to restore the same ATP level of untreated cells (supporting information Figure S8), potentially suggesting a different mechanism of action for these compounds. On the other hand, the naphthoquinones showed low toxicity in SH-SY5Y and HepG2 cell lines (Table 3). In particular, Idebenone showed significant cytotoxicity in NQO1 deficient cell line, while **49** did not show a particular cytotoxic effect in both cell lines even at 100 μ M (supporting information Figure S8).

Cytoprotection on mouse retina explants

Although **1**, **49** and **58** showed a lower efficacy than idebenone, they demonstrated a higher potency and a low cytotoxic profile in SH-SY5Y cells. We therefore decided to test the most active compounds using mouse retina explants to assess if they were able to rescue rotenone-induced retinal ganglion cell loss. In our previous study, we found that NQO1 was predominantly present in the retinal ganglion cell (RGC) layer suggesting the quinones can be metabolized into hydroquinones cells present in that layer¹⁷. Moreover, idebenone was able to switch from an antioxidant to a pro-oxidant, depending on its concentration and NQO1 expression: 10 μ M idebenone showed a significant cell rescue under complex I impairment by increasing cell survival from 41 to 73%, while 20 μ M idebenone caused significant toxicity in the RGC layer. To test the hypothesis that the naphthoquinones identified in this

study could provide protection against RGC loss caused by complex I dysfunction, **1** was tested on retina explants to assess their rescue rotenone-induced RGC loss, using the same procedure applied previously¹⁷.

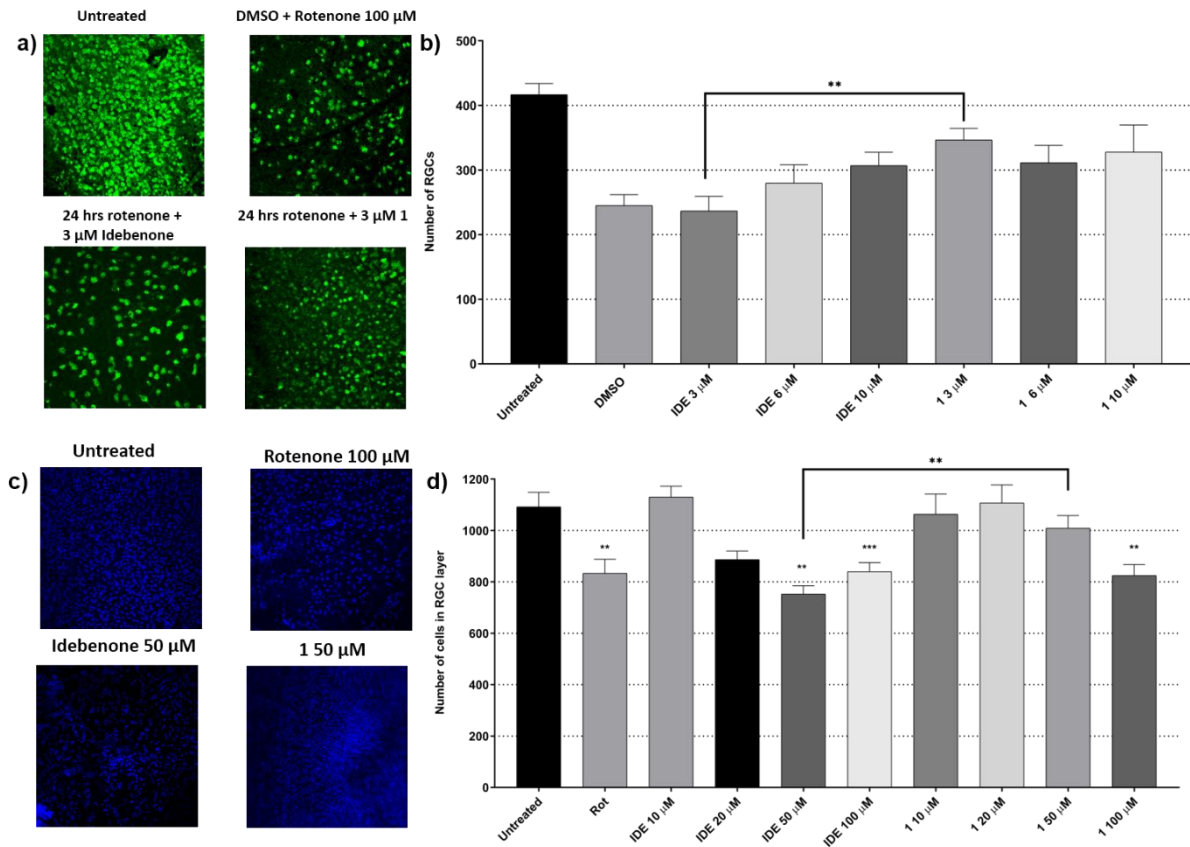


Figure 15 Treatment of retinal explants with **1** and idebenone. **a** Representative *en face* images of RNA-binding protein with multiple splicing (RBPMS) positive cells in the central retina incubated with 100 μ M rotenone and either 3 μ M of idebenone or 3 μ M of **1**. The graph **b** shows mean numbers of RGCs in the central retina after 24 h incubation ex vivo. There is a significant reduction ($p \leq 0.001$) in the number of RGCs in retinae treated with 100 μ M rotenone (DMSO) compared to those treated with the 0.01% DMSO vehicle (untreated). The number of RGCs is significantly higher in explants treated with 100 μ M rotenone and 3 μ M **1** compare to those treated with 3 μ M idebenone. **c** Representative *en face* images of Hoechst nuclear stain in the ganglion cell layer from the central retina of explants incubated with 50 μ M idebenone (IDE), or 50 μ M **1** for 24 h. 100 μ M rotenone (Rot) was used as positive control. The graph **d** shows the mean number of cells per area in the retinal ganglion cell layer (RGC) of the central retina after 24 h ex vivo. No cell loss is seen after 24 h ex vivo with 50 μ M **1** compared to those treated with Idebenone. Error bars represent \pm SEM. Data were analyzed using 1-way ANOVA, Tukey multiple comparison tests, P values were calculated versus untreated cells (DMSO vehicle) (** $p \leq 0.01$, *** $p \leq 0.001$)

Interestingly, the results showed that **1** not only has proved superior therapeutic efficacy compared to idebenone, almost completely rescuing the retinal ganglion cells, but it also provides a better cytotoxicity profile, showing a reduction on the number of cells in the RGC layer only at higher concentration (Figure 15). This difference in the activity might be explained by a higher potency at a lower concentration than idebenone and/or better drug permeability, and better NQO1 targeting than idebenone, which might be responsible for the reduced toxicity in the cell populations in the retinal ganglion cell layer, characterized by a lower or no NQO1 presence.³²

Conclusion

In conclusion, we successfully obtained novel naphthoquinones structures based on the 2- amine 1,4 naphthoquinone scaffolds and found that some of them had potent ATP rescue activity under complex I inhibition toward NQO1-complex III pathway. The SARs shown in this study provided a more comprehensive understanding of the specific features for the activity, including the aniline substituent in position 2 and the presence of a mild EDG which might affect the electronic behaviour and consequently the potential reduction of the molecule. Despite the structural similarity with Woolley's compounds, here we showed that the presence of an anile group directly linked to the core might increase the affinity for NQO1 rather than other oxidoreductases, and the lack of NQO1 expression in cells such as SH-SY5Y showed a totally lost of the activity (supporting information Figure S9). In addition, **1** demonstrated superior efficacy and safety to idebenone on retinal explants and thus is believed to be a particularly good candidate for *in vivo* studies. In fact, pharmacokinetic and metabolic studies of idebenone showed a low bioavailability of parent Idebenone, with an intraocular concentration of 111 nM in the aqueous humour after a single oral administration of 60 mg/kg of idebenone to male mice^{33,34}. The *in vitro* metabolic stability studies showed a slightly longer half-life of **1** than Idebenone (supporting information Table S1). According to these data, the novel identified compounds **1** and **49**, might be within the therapeutic range shown to be more effective in protecting cells from complex I impairment than idebenone, and with lower toxic side effects.

EXPERIMENTAL SECTION

General.

All reagents and anhydrous solvents were used as obtained from commercial sources without further purification. Reactions were monitored by thin layer chromatography using silica gel 60 F254 plates and staining were visualized by irradiation with UV light at 254 nm and 366 nm. The final products and intermediates of reactions were purified by recrystallization in ethanol or flash column

chromatography (Biotage Isolera™ Prime with SNAP Cartridges KP-Sil column.). The purity of synthesized compounds was assessed by UPLC-MS; meanwhile, the presence of residual solvent was assessed by NMR. UPLC-MS analysis was conducted on a Waters UPLC system with both diode array absorption detection of UV-visible light, and Electrospray (+ve and -ve ion) MS detection. The stationary phase was a Waters Acquity UPLC BEH C18 1.7 μ m 2.1x50mm column. The mobile phase was H₂O containing 0.1% Formic acid (A) and MeCN containing 0.1% Formic acid (B). Column temperature: 40°C. Sample diluent: acetonitrile. Sample concentration 10 μ g/mL. Injection volume 2 μ L. Three methods were used: linear gradient standard method A: 90% A (0.1 min), 90%-0% A (2.6 min), 0% A (0.3 min), 90% A (0.1 min); flow rate 0.5 mL/min. Linear gradient standard method B: 90% A (0.1 min), 90%-0% A (2.1 min), 0% A (0.8min), 90% A (0.1 min); flow rate 0.5 mL/min. Linear gradient standard method C: 90% A (0.1 min), 90%-0% A (1.5 min), 0% A (1.4min), 90% A (0.1 min); flow rate 0.5 mL/min. Unless otherwise stated, all compounds were >95% pure as determined by UPLC. ¹H and ¹³C NMR spectra were recorded on a Bruker AVANCE 500 spectrometer (500 MHz and 75 MHz respectively and auto-calibrated to the deuterated solvent reference peak. Chemical shifts are given in δ relative to tetramethylsilane (TMS); the coupling constants (*J*) are given in Hertz.

General procedure 1: synthesis of 2-chloro-3-amino derivatives

A mixture of 2,3-dichloronaphthoquinone and the corresponding amine (1.5 eq) in absolute ethanol was stirred at room temperature and monitored by TLC until completion. The resulting mixture was concentrated in vacuum, and the residue was partitioned between a HCl 1 N solution and AcOEt. The organic layer was dried over anhydrous magnesium sulphate, filtered and concentrated. The crude product was purified using silica gel column chromatography, Biotage Isolera One system, using nHexane/EtOAc as eluent to afford the pure compound. In some reactions, the pure precipitated product was collected by vacuum filtration

General procedure 2: synthesis of 2-alkoxy-3-chloro naphthoquinones

A mixture of 2,3-dichloronaphthoquinone, the corresponding alcohol (1.2 eq) and K₂CO₃ (1.2 eq) in THF (0.2 M) was stirred at room temperature for 12 h. The resulting mixture was concentrated in vacuum, and the residue was partitioned between a HCl 1N solution and AcOEt. The combined organic layers were dried over anhydrous magnesium sulfate, filtered and concentrated. The crude product was purified using silica gel column chromatography Biotage Isolera One system, using nHexane/EtOAc as eluent to afford the pure compound. When possible, the pure precipitated product was collected by vacuum filtration without further purification

General procedure 3: Microwave-assisted Buchwald–Hartwig amination

A microwave tube-with a magnetic stir bar was charged with t-BuOK (1.5 eq) naphthoquinone (1.0 eq), XPhos (10 mol %), Pd₂(dba)₃ (10 mol %) and the appropriate aniline (1.5 eq), sealed with a septum, and degassed by alternating vacuum evacuation and nitrogen (three times) before anhydrous toluene (0.3 M) was added by a syringe. The reaction mixture was irradiated at the MW for 30 min at 130°C. After the reaction was complete, the mixture was dissolved in AcOEt, filtered on Celite and washed with HCl 2 N. The organic layer was dried over anhydrous magnesium sulfate, filtered and concentrated. The crude product was purified using silica gel column chromatography, Biotage Isolera One system, using nHexane/EtOAc as eluent to afford the final compound.

General procedure 4 synthesis of 2-sulfanyl -3-benzammine naphthoquinones

To a mixture of 2-chloro-3-((3-(trifluoromethyl) phenyl) amino) naphthalene-1,4-dione (1 eq) in EtOH appropriate Thiols (2 eq) and K₂CO₃ (2 eq) were added, and the reaction was stirred at room temperature. The resulting mixture was concentrated in vacuum, and the residue was partitioned between water and AcOEt. The combined organic layers were dried over anhydrous magnesium sulfate, filtered and concentrated. The crude product was purified using silica gel column chromatography, Biotage Isolera One system, using nHexane/EtOAc as eluent to afford the final compound.

General procedure 5: synthesis of 2-aminonaphthalene-1,4-dione

The 1,4 naphthoquinone (1.0 eq) was stirred with cerium trichloride heptahydrate (1.5 eq) in EtOH at room temperature. After 15 minutes, the appropriate aniline (1.5 eq) was added, and the reaction was stirred for 12 h. The resulting mixture was concentrated in vacuum, and the residue was partitioned between satd. aq. NH₄Cl and AcOEt. The combined organic layers were washed with HCl 6N and dried over anhydrous magnesium sulfate, filtered and concentrated. The crude product was purified using silica gel column chromatography, Biotage Isolera One system, using Hexane/EtOAc as eluent to afford the final compound. In some reactions, the pure precipitated product was collected by vacuum filtration.

General procedure 6: synthesis of 2-chloro-3-aminonaphthalene-1,4-dione

The 2-chloronaphthalene-1,4-dione (1.0 eq) was stirred with cerium trichloride heptahydrate (1.5 eq) in EtOH at room temperature. After 15 minutes, the appropriate aniline (1.5 eq) was added, and the reaction was stirred for 24 h at 60°C. The reaction mixture was cooled, and the precipitated was collected by vacuum filtration.

General procedure 8: synthesis of 2-chloro-3-aminonaphthalene-1,4-dione

A Schlenk tube equipped with a magnetic stir bar was charged with naphthoquinones (1.0 eq), $\text{Cu}_2(\text{OH})_2\text{CO}_3 \cdot \text{H}_2\text{O}$ (1.5 eq), AgSCF_3 (3.0 eq) and $\text{K}_2\text{S}_2\text{O}_8$ (3.0 eq). The tube was sealed with a septum, and degassed by alternating vacuum evacuation and nitrogen (three times) before anhydrous CH_3CN (0.3 M) was added by a syringe. The mixture was stirred at 65 °C overnight for 12 h. The solution was then cooled to room temperature and a satd. aq. NH_4Cl solution was added. The resulting mixture was filtered by Celite, eluted with DCM. Separated the organic layers, the water phase was extracted with DCM two times. The combined organic phases were dried over anhydrous magnesium sulfate, filtered and concentrated. The crude product was purified using silica gel column chromatography, Biotage Isolera One system, using nHexane/EtOAc as eluent to afford the final compound.

2-((4-fluoro-3-(trifluoromethyl)phenyl)amino)-3-(methylthio)naphthalene-1,4-dione (1) The title compound was obtained according to the general procedure 6. **Yield:** 80 %, **State:** red solid. **UPLC-MS** method C: 2.46 MS (ESI)+: 382[M+H]⁺. **¹H-NMR (500 MHz, CDCl_3)** δ : 8.28-8.23 (m, 1H), 8.20 – 8.12 (m, 1H), 7.82 (td, J = 1.4, 7.6 Hz, 1H), 7.76 (td, J = 1.3, 7.5 Hz, 1H), 7.54 – 7.48 (m, 1H), 7.45 (s, 1H), 7.39 (dd, J = 2.3, 7.3 Hz, 1H), 7.28 – 7.24 (m, 1H). **¹³C-NMR (125 MHz CDCl_3)**, 180.9, 180.3, 142.9, 138.6, 134.7, 134.7, 133.4, 133.3, 133.1, 131.5, 130.7, 128.9, 126.7, 124.8, 124.6, 121.6, 120.6, 16.8.

2-amino-3-chloronaphthalene-1,4-dione (23) The title compound was obtained according to the general procedure 1 **Yield** 78%, **State:** orange solid **UPLC-MS** method C: Rt: 1.56 MS (ESI)+: 308.0-210.0 [M+H]⁺ **¹H-NMR (500 MHz, CDCl_3)** δ 7.99 – 7.95 (m, 2H), 7.82 (td, J = 7.5, 1.4 Hz, 1H), 7.74 (td, J = 7.5, 1.3 Hz, 1H), 7.32 (s, 3H).

2-chloro-3-((3,3,3-trifluoropropyl)amino)naphthalene-1,4-dione (24) The title compound was obtained according to the general procedure 1 **Yield** 88% **State:** red solid **UPLC-MS** method C: 2.21 MS (ESI)+: 304.2[M+H]⁺ **¹H-NMR (500 MHz, CDCl_3)** δ 8.09 (dd, J = 7.7, 1.3 Hz, 1H), 8.05 – 7.98 (m, 1H), 7.70 – 7.64 (m, 1H), 7.59 (dd, J = 7.6, 1.3 Hz, 1H), 6.07 (s, 1H), 4.06 (q, J = 6.8 Hz, 3H), 2.47 (dt, J = 10.5, 6.7 Hz, 2H). **¹³C-NMR (125 MHz CDCl_3)**, δ 176.6, 135.3, 132.1, 126.9, 38.05, 35.6.

2-chloro-3-((3-Chlorobenzyl) amino) naphthalene-1,4-dione (25) The title compound was obtained according to the general procedure 1 **Yield** 73% **State:** red solid **UPLC-MS** method B: Rt: 2.71, MS (ESI)+: 332.1-334.1[M+H]⁺ **¹H-NMR (500 MHz, CDCl_3)** δ 8.23-8.21 (m, 1H), 8.18 (d, J =7.7, Hz 1H), 8.08 (d, J = 7.6, Hz, 1H), 7.64– 7.62 (m, 1H), 7.76 (dt, J = 6.3, 1.4 Hz, 1H), 7.66 (t, J = 7.7, 1.2 Hz, 1H), 7.34-7.33 (m, 1H), 7.23-7.22 (m, 1H), 5.05 (s, 2H) **¹³C-NMR (125 MHz CDCl_3)** δ : 176.9, 176.1, 140.1, 135.0, 134.8, 134.7, 132.7, 132.5, 130.3, 129.7, 128.2, 127.8, 127.6, 126.9, 125.6, 48.1.

2-chloro-3-((3-(trifluoromethyl) benzyl) amino) naphthalene-1,4-dione (26) The title compound was obtained according to the general procedure 1 **Yield** 66% **State** : red solid **UPLC-MS** method B: Rt: 2.31, MS (ESI)-: 364.2-366.2[M-H]⁻ **¹H-NMR (500 MHz, CDCl₃) δ**: 8.20(dd, J=7.78,1.0 1H), 8.09 (dd, J = 7.7, 1.1, 1H), 7.79 (dt, J = 7.6, 1.3 Hz, 1H), 7.60 (dt, J = 7.64,1.1 Hz, 1H), 7.20 (m, 1H),7.62-7.60 (m, 2H), 7.56-7.54 (m, 2H), 6.28(bs, 1H) 5.15 (dd, 1H) **¹³C-NMR (125 MHz CDCl₃), δ**: 180.4, 176.6, 143.4, 135.1, 132.2, 132.6, 129.9, 126.2, 127.8, 127.0, 126.8, 48.2.

2-chloro-3-((3-(methylthio) benzyl) amino) naphthalene-1,4-dione (27) The title compound was obtained according to the general procedure 1 **Yield** 44% **Purity**:92% **State** orange solid **UPLC-MS** method B: Rt: 2.71, MS (ESI)+: 344.2-146. [M+H]⁺ **¹H-NMR (500 MHz, CDCl₃) δ**: 8.13-8.11 (m, 1H), 8.08 (d, J = 7.7, 1, 1H), 7.97 (d, J = 7.8 Hz, 1H), 7.75-7.73 (m, 1H), 7.67 (dt, J = 7.1, 1.1 Hz, 1H), 7.57 (dt, J = 7.8,1.1 Hz, 1H), 7.20 (m, 1H),7.23-7.22 (m, 1H), 4.94 (s, 2H), 4.67 (s, 3H) **¹³C-NMR (125 MHz CDCl₃), δ**: 180.4, 176.1, 138.5, 134.9, 134.6, 134.6, 132.6, 130.9, 128.2, 127.8, 127.1, 126.8, 58.4, 18.4.

2-chloro-3-((1-phenylethyl) amino) naphthalene-1,4-dione (28) The title compound was obtained according to the general procedure 1 **Yield** 35% **State** red solid **UPLC-MS** method B: Rt: 2.45, MS (ESI)+: 312.1-314.1 [M+H]⁺ **¹H-NMR (500 MHz, CDCl₃) δ**: 8.15 – 7.95 (m, 2H), 7.95 (dd, J = 7.7, 0.8 Hz, 1H), 7.64 – 7.56 (m, 1H), 7.56 – 7.46 (m, 1H), 7.31 – 7.25 (m, 2H), 7.20 (dt, J = 7.0, 2.4 Hz, 1H), 5.80 – 5.65 (m, 1H), 1.57 (d, J = 6.7 Hz, 3H). **¹³C-NMR (125 MHz CDCl₃), δ**: 180.5, 176.9, 143.8, 134.9, 132.6, 132.5, 129.8, 128.9, 127.6, 126.9, 125.7, 53.4, 24.6.

2-chloro-3-(phenethylamine) naphthalene-1,4-dione (29) The title compound was obtained according to the general procedure 1 **Yield** 76% **State**: red solid **UPLC-MS** method B: Rt: 2.46, MS (ESI)+: 312.2-314.1 [M+H]⁺ **¹H-NMR (500 MHz, CDCl₃) δ** 8.17 (dd, J = 7.7, 0.8 Hz, 1H), 8.04 (dd, J = 7.7, 0.9 Hz, 1H), 7.75 (td, J = 7.6, 1.3 Hz, 1H), 7.64 (td, J = 7.6, 1.2 Hz, 1H), 7.36 (t, J = 7.3 Hz, 2H), 7.27 (d, J = 8.1 Hz, 2H), 6.12 (s, 1H), 4.15 (dd, J = 13.9, 6.9 Hz, 2H), 3.02 (t, J = 7.2 Hz, 2H). **¹³C-NMR (125 MHz CDCl₃), δ**:180.4, 137.7, 134.9, 134.7, 132.7, 132.4, 128.9, 128.8, 127.8, 126.9, 126.8, 126.8, 46.0, 37.3.

2-chloro-3-((3-(trifluoromethyl)phenethyl)amino)naphthalene-1,4-dione (30) The title compound was obtained according to the general procedure 11 **Yield** 82% **State**: red solid **UPLC-MS** method C: 2.49 MS (ESI)+: 380[M+H]⁺ **¹H-NMR (500 MHz, CDCl₃) δ**(500 MHz, Chloroform-d) 8.09 (dd, J = 7.6, 0.5 Hz, 1H,), 7.96 (dd, J = 7.7, 1.4, 1H,), 7.67 (td, J = 7.6, 1.4 Hz, 1H), 7.57 (td, J = 7.6, 1.3 Hz, 1H), 7.48 – 7.35 (m, 4H), 6.00 (s, 1H), 4.06 (dt, J = 7.4, 6.5 Hz, 2H), 2.99 (t, J = 7.2 Hz, 2H).

2-chloro-3-(phenylamino) naphthalene-1,4-dione (31) The title compound was obtained according to the general procedure 1 **Yield** 76% **State**: red solid **UPLC-MS** method B: Rt: 2.54, MS (ESI)+: 284.0-285.8[M-H]⁺ **¹H-NMR (500 MHz, CDCl₃) δ**: : 8.09(d, J=7.67,1.0 1H), 7.97 (dd, J = 7.44, 1.1, 1H), 7.68 (dt,

J = 8.2, Hz, 1H), 7.57 (t, J = 6.86, 1.1 Hz, 1H), 7.20 (m, 1H), 7.33-7.30 (m, 2H), 7.27-7.26 (m, 2H), 6.15 (bs, 1H) ¹³C-NMR (125 MHz CDCl₃), δ: 180.4, 137.9, 134.95, 132.6, 132.5, 129.8, 129.1, 128.1, 127.7, 126.8.

2-chloro-3-((3-hydroxyphenyl)amino) naphthalene-1,4-dione (32) The title compound was obtained according to the general procedure 1 **Yield** 15% **Purity:** 94 % **State:** purple solid **UPLC-MS** method B: Rt: 1.94, MS (ESI)⁺: 280.04[M+H]⁺ ¹H-NMR (500 MHz, CDCl₃) δ: 9.08(s, 1H), 8.11-8.09 (m, 1H), 8.05-8.02 (m, 1H), 7.93-7.90 (m, 1H), 7.87 (dt, J = 6.58, 1.51 Hz, 1H), 7.82 (dt, J = 7.31, 1 Hz, 1H), 7.72(t, J=7.7, 1H), 7.10(t=7.1 1H), 6.74-6.70(m, 1H) ¹³C-NMR (125 MHz CDCl₃), δ: 180.4, 137.8, 134.9, 132.6, 129.6, 129.1, 128.1, 127.7, 126.7, 125.6.

2-chloro-3-((3-(trifluoromethyl) phenyl) amino) naphthalene-1,4-dione (33) The title compound was obtained according to the general procedure 1 **Yield** 66% **State:** red solid **UPLC-MS** method B: Rt: 2.31 MS (ESI)⁺: 352.2-354.1[M+H]⁺ ¹H-NMR (500 MHz, CDCl₃) δ: 7.94-7.92(m, 1H), 7.66-7.62 (m, 2H), 7.53 (s, 1H), 7.49-7.45 (m, 2H), 7.36-7.35 (m, 2H), ¹³C-NMR (125 MHz CDCl₃), δ: 178.4, 147.6, 134.7, 134.3, 134.2, 132.5, 129.6, 127.8, 127.4, 124.8, ¹⁹F NMR (471 MHz, CDCl₃) δ -62.82.

2-chloro-3-((4-(trifluoromethyl) phenyl) amino) naphthalene-1,4-dione (34) The title compound was obtained according to the general procedure 1 **Yield** 40% **State:** red solid **UPLC-MS** method B: Rt: 2.41 MS (ESI)⁺: 352.2-354.4[M+H]⁺ ¹H-NMR (500 MHz, CDCl₃) δ: 8.25(d, J=6.42 1H), 8.18 (d=7.25, 2H), 7.83 (dt, J = 7.7 Hz, 1H), 7.78 (dt, J = 7.7, 1 Hz, 1H), 7.66 (d, J=7.9, 2H), 7.16(d, J=8.2 2H) ¹³C-NMR (125 MHz CDCl₃), δ: 180.1, 176.2, 138.5, 134.4, 132.5, 132.6, 130.6, 130.9, 129.2, 127.8, 127.3, 126.8, 125.6.

2-chloro-3-((4-propylphenyl) amino) naphthalene-1,4-dione (35) The title compound was obtained according to the general procedure 1 **Yield** 38%, **purity:** 90% **State:** red solid **UPLC-MS** method B: Rt: 2.70, MS (ESI)⁺: 326.2-328.2 [M+H]⁺ ¹H-NMR (500 MHz, CDCl₃) δ 8.14-8.12 (m, 2H), 7.85-7.83(m, 1H), 7.79 (dt, J = 7.5, 1.70 Hz, 1H), 7.72 (dt, J = 7.4, 1.4 Hz, 1H), 7.19 (d, J=7.9, 2H), 7.16(d, J=8.8 2H), 2.63(t, J=7.8), 1.72-1.60(m, 2H), 0.99(d, J=7.3) ¹³C-NMR (125 MHz CDCl₃), δ: 177.4, 140.5, 135.0, 134.7, 132.9, 132.7, 129.9, 128.4, 127.8, 127.1, 127.0, 124.3, 124.1, 37.5, 24.5, 13.8.

2-chloro-3-((3-(2-hydroxyethyl) phenyl) amino) naphthalene-1,4-dione (36) Compound was obtained according to the general procedure 1 **Yield** 31% **State:** red solid **UPLC-MS** method B: Rt: 1.96, MS (ESI)⁺: 328.2-330.2[M+H]⁺ ¹H-NMR (500 MHz, CDCl₃): 8.22 (dd, J = 7.7, 0.9 Hz, 1H), 8.14 (dd, J = 7.6, 0.9 Hz, 1H), 7.78 (td, J = 26.4, 16.3, 1.3 Hz, 1H), 7.76 – 7.59 (m, 2H), 7.24 (d, J = 8.3 Hz, 2H), 7.06 (d, J = 8.2 Hz, 2H), 3.91 (t, J = 6.5 Hz, 2H), 2.92 (t, J = 6.5 Hz, 2H). ¹³C-NMR (125 MHz CDCl₃), δ: 180.5, 177.4, 141.5, 136.2, 135.8, 135.1, 133.0, 132.6, 129.9, 129.0, 127.1, 127.0, 124.5, 63.5, 38.7.

2-chloro-3-(3-methyl-4-phenoxyphenoxy) naphthalene-1,4-dione (37) The title compound was obtained according to the general procedure 1 **Yield** 32%, **purity** 94% **State:** red solid **UPLC-MS** method

B: Rt: 2.70, MS (ESI)+: 391.4-393.4[M+H]⁺ ¹H-NMR (500 MHz, CDCl₃) δ: 8.14 (dd, J = 7.7, 0.9 Hz, 1H), 8.07 (dd, J = 7.7, 0.9 Hz, 1H), 7.72 (td, J = 7.6, 1.3 Hz, 1H), 7.65 (td, J = 7.6, 1.3 Hz, 1H), 7.54 (s, 1H), 7.34 (d, J = 2.6 Hz, 1H), 7.31 – 7.23 (m, 2H), 7.10 (dd, J = 8.8, 2.7 Hz, 1H), 6.96 – 6.89 (m, 2H), 6.84 (d, J = 8.8 Hz, 1H), 1.47 (s, 3H) ¹³C-NMR (125 MHz CDCl₃), δ: 179.5, 138.5, 135.2, 133.4, 133.2, 130.0, 129.0, 127.3, 127.1, 123.3, 120.5, 119.2, 17.3.

2-chloro-3-((4-methoxy-3-(trifluoromethyl) phenyl) amino) naphthalene-1,4-dione (38) The title compound was obtained according to the general procedure 1 **Yield** 34% **State:** red solid **UPLC-MS** method B: Rt: 2.41, MS (ESI)+: 382.2-384.1[M+H]⁺ ¹H-NMR (500 MHz, CDCl₃) δ: 8.24 (d, J=7.11H), 8.16 (d=7.05, 2H), 7.81 (dt, J = 7.7 Hz, 1H), 7.73 (dt, J = 7.7, 1 Hz, 1H), 7.62 (bs, 1H), 7.37 (d, J=7.9, 2H), 7.26 (d, J=8.2 1H), 3.97 (s, 1H) ¹³C-NMR (125 MHz CDCl₃), δ: 180.3, 179.0, 138.5, 135.15, 133.04, 129.54, 127.21, 127.04, 123.92, 111.87, 56.27.

2-chloro-3-((4-fluoro-3-(trifluoromethyl)phenyl)amino)naphthalene-1,4-dione(39) The title compound was obtained according to the general procedure 1 **Yield** 34% **State:** red solid **UPLC-MS** **MS** method C: 2.06 MS (ESI)+: 370-372[M+H]⁺ ¹H-NMR (500 MHz, CDCl₃) δ: 8.18 – 8.10 (m, 1H), 8.07 (dd, J = 7.7, 1.4 Hz, 1H), 7.76 – 7.70 (m, 1H), 7.66 (td, J = 7.6, 1.4 Hz, 1H), 7.52 (s, 1H), 7.26 (dd, J = 6.1, 2.7 Hz, 1H), 7.18 – 7.10 (m, 1H). ¹³C-NMR (125 MHz CDCl₃) δ: 180.16, 176.62, 141.19, 135.28, 133.69, 133.31, 132.69, 132.37, 129.73, 129.48, 127.15, 126.35, 122.90, 116.97, 103.84.

2-hydroxy-3-(phenylamino)naphthalene-1,4-dione (40) The title compound was obtained according to the general procedure 3 **Yield** 76% **State:** purple solid **UPLC-MS** method C: 1.14 MS (ESI)+: 266[M+H]⁺ ¹H-NMR (500 MHz, CDCl₃) δ: 8.13 (dd, J = 7.7, 1.4 Hz, 1H), 8.05 (dd, J = 7.7, 1.4 Hz, 1H), 7.68 (dd, J = 7.6, 1.4 Hz, 1H), 7.65 (dd, J = 7.6, 1.4 Hz, 1H), 7.28 (dd, J = 8.5, 7.4 Hz, 2H), 7.15 (s, 1H), 7.15 – 7.08 (m, 1H), 7.08 – 7.02 (m, 2H) ¹³C-NMR (125 MHz CDCl₃), δ: 183.2, 179.7, 139.4, 138.7, 134.6, 133.8, 132.7, 132.2, 130.1, 128.3, 126.3, 126.2, 124.1, 122.2, 59.92.

2-methoxy-3-(phenylamino) naphthalene-1,4-dione (41) The title compound was obtained according to the general procedure 3 **Yield** 80% **State:** orange solid **UPLC-MS** method C: 1.15 MS (ESI)+: 280[M+H]⁺ ¹H-NMR (500 MHz, CDCl₃) δ: 8.11 (dd, J = 7.7, 1.4 Hz, 1H), 8.07 (dd, J = 7.7, 1.4 Hz, 1H), 7.72 (dd, J = 7.6, 1.4 Hz, 1H), 7.66 (dd, J = 7.6, 1.4 Hz, 1H), 7.31 (dd, J = 8.5, 7.4 Hz, 2H), 7.18 (s, 1H), 7.15 – 7.08 (m, 1H), 7.08 – 7.02 (m, 2H), 3.52 (s, 3H). ¹³C-NMR (125 MHz CDCl₃), δ: 183.2, 179.7, 139.4, 138.7, 134.6, 133.8, 132.7, 132.2, 130.17, 128.31, 126.31, 126.28, 124.06, 122.22, 59.92.

2-ethoxy-3-(phenylamino) naphthalene-1,4-dione (42) The title compound was obtained according to the general procedure 3 **Yield** 64% **State:** orange solid **UPLC-MS** method C: 1.14 MS (ESI)+: 296[M+H]⁺ ¹H-NMR (500 MHz, CDCl₃) δ: : 8.11 (dd, J = 7.6, 1.3 Hz, 1H), 8.07 (dd, J = 7.6, 1.4 Hz, 1H),

7.72 (td, $J = 7.5, 1.3$ Hz, 1H), 7.70 – 7.62 (m, 1H), 7.36 – 7.28 (m, 2H), 7.16 – 6.94 (m, 3H), 3.74 (q, $J = 7.0$ Hz, 2H), 0.85 (t, $J = 7.0$ Hz, 3H). **$^{13}\text{C-NMR}$ (125 MHz CDCl_3)**, δ : 183.3, 179.9, 143.3, 138.6, 134.5, 134.5, 132.6, 132.5, 130.5, 130.3, 128.9, 128.4, 126.2, 125.4, 124.1, 122.8, 68.5, 14.6.

2-(phenylamino)-3-propoxynaphthalene-1,4-dione (43) The title compound was obtained according to the general procedure 3 **Yield** 67% **State**: orange solid **UPLC-MS** method C: 2.45 MS (ESI)+: 308[M+H]⁺ **$^1\text{H-NMR}$ (500 MHz, CDCl_3)** δ : 8.10 (dt, $J = 7.6, 0.9$ Hz, 1H), 8.09 – 8.04 (m, 1H), 7.72 (td, $J = 7.5, 1.3$ Hz, 1H), 7.64 (td, $J = 7.5, 1.4$ Hz, 1H), 7.33 – 7.27 (m, 2H), 7.15 (s, 1H), 7.12 – 7.09 (m, 1H), 7.08 – 7.03 (m, 2H), 3.68 (t, $J = 6.7$ Hz, 2H), 1.36 – 1.22 (m, 2H), 0.65 (t, $J = 7.4$ Hz, 3H).. **$^{13}\text{C-NMR}$ (125 MHz CDCl_3)**, δ : 183.2, 179.8, 143.3, 138.8, 134.5, 132.6, 132.3, 130.5, 130.3, 128.9, 128.2, 126.3, 126.2, 125.6, 123.9, 122.4, 74.6, 22.8, 10.0.

2-isopropoxy-3-(phenylamino) naphthalene-1,4-dione (44) The title compound was obtained according to the general procedure 3 **Yield** 63% **State**: orange solid **UPLC-MS** method C: 1.22 MS (ESI)+: 308[M+H]⁺ **$^1\text{H-NMR}$ (500 MHz, CDCl_3)** δ : 8.11 (dd, $J = 7.6, 1.4$ Hz, 1H), 8.07 (dd, $J = 7.7, 1.4$ Hz, 1H), 7.74 – 7.69 (m, 1H), 7.65 – 7.60 (m, 1H), 7.41 (dd, $J = 5.0, 2.0$ Hz, 1H), 7.33 – 7.28 (m, 2H), 7.20 (bs, 1H), 7.13 – 7.05 (m, 2H), 7.05 – 7.00 (m, 2H), 4.41 – 4.21 (m, 1H), 0.88 (d, $J = 6.1$ Hz, 6H).. **$^{13}\text{C-NMR}$ (125 MHz CDCl_3)**, δ : 181.3, 178.4, 141.4, 136.6, 135.4, 133.1, 132.6, 130.7, 130.3, 128.6, 128.5, 127.1, 126.5, 126.2, 124.4, 124.3, 123.6, 121.9, 120.8, 73.1, 19.9.

2-phenoxy-3-(phenylamino) naphthalene-1,4-dione (45) The title compound was obtained according to the general procedure 3 **Yield** 52% **State**: red solid **UPLC-MS** method C: 2.34 MS (ESI)+: 342[M+H]⁺ **$^1\text{H-NMR}$ (500 MHz, CDCl_3)** δ : 8.18 – 8.11 (m, 1H), 7.82 – 7.71 (m, 2H), 7.69 (dd, $J = 7.6, 1.3$ Hz, 1H), 7.17 (t, $J = 7.8$ Hz, 2H), 7.10 – 7.00 (m, 3H), 6.96 (dd, $J = 7.4, 1.7$ Hz, 2H), 6.90 (dd, $J = 8.7, 1.1$ Hz, 1H), 6.88 – 6.80 (m, 1H), 6.58 – 6.46 (m, 2H). **$^{13}\text{C-NMR}$ (125 MHz CDCl_3)**, δ : 183.5, 179.9, 142.4, 138.9, 135.5, 134.9, 132.7, 129.0, 128.0, 127.6, 127.11, 126.8, 126.5, 125.0, 124.2, 123.7, 121.9, 120.4, 119.3.

2-(methylamino)-3-(phenylamino)naphthalene-1,4-dione (46) The title compound was obtained according to the general procedure 3 **Yield** 45% **State**: purple solid **UPLC-MS** method C: 1.16 MS (ESI)+: 279[M+H]⁺ **$^1\text{H-NMR}$ (500 MHz, CDCl_3)** δ 8.21 – 7.99 (m, 2H), 7.63 (m, 1H), 7.32 – 7.15 (m, 2H), 6.98 – 6.84 (m, 2H), 6.75 (m, 2H), 6.42 (s, 1H) 2.73 (dd, $J = 5.7, 2.5$ Hz, 3H).. **$^{13}\text{C-NMR}$ (125 MHz DMSO)**, δ 181.9, 181.1, 143.6, 137.8, 134.1, 132.6, 132.1, 130.9, 129.0, 128.4, 126.2, 126.1, 120.4, 120.3, 116.5, 113.8, 30.4.

2-(ethylamino)-3-(phenylamino)naphthalene-1,4-dione (47) Compound was obtained according to the general procedure 3 **Yield** 35% **State**: purple solid **UPLC-MS** method C: 1.21 MS (ESI)+: 293v¹ **$^1\text{H-NMR}$ (500 MHz, CDCl_3)** δ : 8.06 – 8.23 (m, 2H), 7.64 -7.62 (m, 2H), 7.43 – 7.41 (m, 2H), 6.98 – 6.84 (m,

2H), 6.42 (s, 1H), 3.14 – 2.96 (m, 2H), 0.96 (t, $J = 7.2$ Hz, 3H). $^{13}\text{C-NMR}$ (125 MHz CDCl_3), δ 188.9, 182.1, 143.3, 143.3, 134.8, 134.0, 133.5, 132.6, 130.5, 128.9, 127.4, 126.3, 126.2, 126.1, 125.4, 37.8, 15.7.

2-(dimethylamino)-3-(phenylamino) naphthalene-1,4-dione (48) The title compound was obtained according to the general procedure 3 **Yield** 49% **State**: purple solid **UPLC-MS** method C: 2.48 MS (ESI)+: 293[M+H] $^{+}$ $^1\text{H-NMR}$ (500 MHz, CDCl_3) δ : 8.09 – 7.89 (m, 2H), 7.62 (m, 2H), 7.39 – 7.18 (m, 2H), 7.19 – 7.06 (m, 1H), 7.04 – 6.95 (m, 1H), 6.91 – 6.71 (m, 2H), 2.74 (s, 6H). $^{13}\text{C-NMR}$ (125 MHz CDCl_3), δ : 182.1, 181.9, 140.2, 133.5, 133.3, 132.7, 130.8, 128.8, 128.2, 127.4, 126.3, 125.5, 121.8, 121.6, 41.0.

2-((4-fluoro-3-(trifluoromethyl)phenyl)amino)-3-methoxynaphthalene-1,4-dione (49) The title compound was obtained according to the general procedure 3 **Yield** 78% **State**: red solid **UPLC-MS** method C: 2.41 MS (ESI)+: 366[M+H] $^{+}$ $^1\text{H NMR}$ (500 MHz, $\text{Chloroform-}d$) δ 8.05 – 8.02 (m, 1H), 8.00 (dt, $J = 7.7$, 0.8 Hz, 1H), 7.68 (td, $J = 7.5$, 1.4 Hz, 1H), 7.60 (td, $J = 7.5$, 1.3 Hz, 1H), 7.21 (dd, $J = 6.0$, 2.8 Hz, 1H), 7.15 – 7.05 (m, 2H), 7.02 (s, 1H), 3.57 (s, 3H). $^{13}\text{C NMR}$ (126 MHz, CDCl_3) δ 182.72, 179.77, 135.20, 134.73, 133.19, 133.00, 130.00, 127.32, 126.44, 120.68, 120.63, 116.84, 60.14.

2-((2-fluoro-5-(trifluoromethyl) phenyl) amino)-3-methoxynaphthalene-1,4-dione (50) The title compound was obtained according to the general procedure 3 **Yield** 72% Purity: 91% **State**: red solid **UPLC-MS** method C: 2.45 MS (ESI)+: 366[M+H] $^{+}$ $^1\text{H-NMR}$ (500 MHz, CDCl_3) δ : 8.07 – 7.95 (m, 1H), 7.72 – 7.64 (m, 1H), 7.62 (dd, $J = 7.5$, 1.4 Hz, 1H), 7.59 – 7.52 (m, 2H), 7.35 (m, 2H), 6.96 (s, 1H), 3.68 (s, 3H). $^{13}\text{C-NMR}$ (125 MHz CDCl_3), δ : 182.3, 179.9, 143.4, 134.8, 134.6, 133.1, 132.3, 131.9, 130.5, 130.0, 128.9, 128.4, 126.4, 126.3, 125.4, 121.5, 120.9, 115.5, 60.2.

2-((4-fluoro-3-(trifluoromethyl) phenyl) amino)-3-(methylamino)naphthalene-1,4-dione (51) The title compound was obtained according to the general procedure 3 **Yield** 72% **State**: purple solid **UPLC-MS** method C: 2.046 MS (ESI)+: 365.2[M+H] $^{+}$ $^1\text{H-NMR}$ (500 MHz, CDCl_3) δ : 8.16 (dd, $J = 7.6$, 1.4 Hz, 1H), 8.10 (dd, $J = 7.6$, 1.4 Hz, 1H), 7.83 (s, 1H), 7.75 (td, $J = 7.5$, 1.4 Hz, 1H), 7.72 – 7.66 (m, 1H), 7.45 (d, $J = 7.9$ Hz, 1H), 7.39 (d, $J = 7.8$ Hz, 1H), 7.26 (d, $J = 3.3$ Hz, 1H), 7.16 (dt, $J = 8.0$, 1.4 Hz, 1H), 2.12 (s, 3H). $^{13}\text{C-NMR}$ (125 MHz CDCl_3), δ 181.61, 180.89, 134.41, 132.99, 131.91, 130.63, 126.49, 126.35, 120.86, 117.48, 117.31, 114.39, 60.41.

2-(methylthio)-3-((3-(trifluoromethyl) phenyl) amino) naphthalene-1,4-dione (52) The title compound was obtained according to the general procedure 4 **Yield** 75% **State**: red solid **UPLC-MS** method C: 2.46 MS (ESI)+: 364[M+H] $^{+}$ $^1\text{H-NMR}$ (500 MHz, CDCl_3) δ : 8.16 (dd, $J = 7.6$, 1.4 Hz, 1H), 8.10 (dd, $J = 7.6$, 1.4 Hz, 1H), 7.83 (s, 1H), 7.75 (td, $J = 7.5$, 1.4 Hz, 1H), 7.72 – 7.66 (m, 1H), 7.45 (d, $J = 7.9$ Hz, 1H), 7.39 (d, $J = 7.8$ Hz, 1H), 7.26 (d, $J = 3.3$ Hz, 1H), 7.16 (dt, $J = 8.0$, 1.4 Hz, 1H), 2.12 (s, 3H). $^{13}\text{C-NMR}$ (125 MHz CDCl_3), δ 180.9, 180.3, 142.9, 138.6, 134.7, 133.4, 133.1, 131.0, 130.8, 130.4, 128.9, 126.8, 124.9, 124.6, 121.6, 120.8, 118.5, 17.9.

2-(ethylthio)-3-((3-(trifluoromethyl) phenyl) amino) naphthalene-1,4-dione (53) The title compound was obtained according to the general procedure 4 **Yield** 73% **State**: red solid **UPLC-MS** method C: 2.53 MS (ESI)+: 378[M+H]⁺ **¹H-NMR (500 MHz, CDCl₃)** δ 8.09 (dd, J = 7.6, 1.3 Hz, 1H), 8.03 (dd J = 7.6, 1.5 Hz, 1H), 7.74 (s, 1H), 7.68 (td, J = 7.6, 1.4 Hz, 1H), 7.67 – 7.59 (m, 1H), 7.38 (t, J = 7.8 Hz, 1H), 7.32 (d, J = 7.8 Hz, 1H), 7.09 (dt, J = 8.1, 1.5 Hz, 1H), 2.57 (d, J = 7.4 Hz, 2H), 0.98 (t, J = 7.4 Hz, 3H). **¹³C-NMR (125 MHz CDCl₃)**, δ 181.1, 180.2, 144.1, 138.9, 134.7, 133.4, 133.1, 130.5, 128.9, 127.0, 126.8, 125.0, 120.9, 119.9, 118.8, 28.0, 14.4.

2-(isopropylthio)-3-((3-(trifluoromethyl) phenyl) amino) naphthalene-1,4-dione (54) The title compound was obtained according to the general procedure 4 **Yield** 69% **State**: red solid **UPLC-MS** method C: 2.58 MS (ESI)+: 378[M+H]⁺ **¹H-NMR (500 MHz, CDCl₃)** δ: δ 8.09 (dd, J = 7.8, 1.4 Hz, 1H), 8.01 (dd, J = 7.7, 1.4 Hz, 1H), 7.77 (s, 1H), 7.68 (td, J = 7.6, 1.4 Hz, 1H), 7.61 (td, J = 7.5, 1.4 Hz, 1H), 7.35 (dd, J = 20.3, 7.8 Hz, 2H), 7.09 (dt, J = 7.6, 1.6 Hz, 1H), 1.00 (d, J = 6.7 Hz, 6H). **¹³C-NMR (125 MHz CDCl₃)**, δ: δ 181.1, 180.2, 145.1, 139.0, 134.6, 133.3, 133.0, 130.7, 128.9, 127.0, 126.8, 125.6, 121.1, 119.3, 37.9, 24.

2-((2-fluoro-5-(trifluoromethyl) phenyl) amino)-3-(methylthio) naphthalene-1,4-dione (55) The title compound was obtained according to the general procedure 4 **Yield**: 63 % **State**: red solid **UPLC-MS** method C: 2.48 MS (ESI)+: 382[M+H]⁺ **¹H-NMR (500 MHz, CDCl₃)** δ 8.08 (dd, J = 7.6, 1.3 Hz, 1H), 8.03 (dd, J = 7.7, 1.4 Hz, 1H), 7.77 – 7.65 (m, 2H), 7.63 (dd, J = 7.6, 1.4 Hz, 1H), 7.10 (dd, J = 7.7, 1.5 Hz, 2H), 2.07 (s, 3H). **¹³C-NMR (125 MHz CDCl₃)**, δ: 180.8, 180.2, 143.5, 135.3, 134.8, 133.4, 133.1, 130.3, 127.3, 126.8, 120.6, 117.0, 116.8, 17.4.

2-((3-(trifluoromethyl) phenyl) amino)-3-((trifluoromethyl)thio) naphthalene-1,4-dione (56) Compound was obtained according to the general procedure 8 **Yield** 70%. **State**: yellow solid **UPLC-MS** method C: 2.48 MS (ESI)+: 418[M+H]⁺ **¹H-NMR (500 MHz, CDCl₃)** δ: 8.20 (dd, J = 7.8, 1.3 Hz, 1H), 8.15 (s, 1H), 8.11 (dd, J = 7.7, 1.3, 1H), 7.78 (td, J = 7.6, 1.4 Hz, 1H), 7.68 (td, J = 7.6, 1.3 Hz, 1H), 7.55 – 7.51 (m, 1H), 7.48 (t, J = 7.8 Hz, 1H), 7.36 (d, J = 1.9 Hz, 1H), 7.28 (dd, J = 7.9, 1.9 Hz, 1H). **¹³C-NMR (125 MHz CDCl₃)**, δ: δ 180.3, 179.8, 150.4, 138.5, 135.8, 133.2, 133.1, 129.9, 129.8, 128.9, 127.7, 127.3, 124.1, 122.8.

2-((4-fluoro-3-(trifluoromethyl) phenyl) amino)-3-((trifluoromethyl)thio) naphthalene-1,4-dione (57) The title compound was obtained according to the general procedure 8 **Yield** 64%, purity 90%. **State**: yellow solid **UPLC-MS** method C: 2.48 MS (ESI)+: 436[M+H]⁺ **¹H-NMR (500 MHz, CDCl₃)** δ: δ 8.19 (dd, J = 7.7, 1.3 Hz, 1H,), 8.14 – 8.02 (m, 2H,), 7.78-7.76 (m, 2H,), 7.70-7.66 (m, 1H,), 7.37-7.35 (m, 1H,), 7.30-7.27 (d, J = 3.5 Hz, 2H,). **¹³C-NMR (125 MHz CDCl₃)**, δ: 180.1, 179.7 159.4, 157.3, 150.5, 135.8, 134.8, 133.9, 133.9, 133.3, 133.0, 131.5, 129.9, 127.8, 127.3, 117.9, 117.8.

2-((4-fluoro-3-(trifluoromethyl)phenyl)amino)-3-methylnaphthalene-1,4-dione (58) Compound was obtained according to the general procedure 7 **Yield** 83%. **State:** orange solid **UPLC-MS** method C: 2.41 MS (ESI)⁺: 366[M+H]⁺ **¹H-NMR (500 MHz, Chloroform-d)** δ 8.07 (ddd, J = 7.7, 1.4, 0.5 Hz, 1H), 8.03 (ddd, J = 7.7, 1.4, 0.5 Hz, 1H), 7.68 (td, J = 7.5, 1.4 Hz, 1H), 7.62 (dd, J = 7.5, 1.4 Hz, 1H), 7.26 (s, 1H), 7.15 – 7.02 (m, 3H), 1.68 (s, 3H). **¹³C-NMR (126 MHz, CDCl₃)** δ 184.45, 182.19, 142.05, 136.23, 134.67, 133.03, 132.79, 130.32, 126.56, 126.37, 120.32, 120.12, 14.06.

2-chloro-3-hydroxynaphthalene-1,4-dione (60) The title compound was obtained according to the general procedure 2 **Yield** 83% **State:** purple solid **UPLC-MS** method C: Rt: 1.47, MS (ESI)⁺: 208[M+H]⁺ **¹H-NMR (500 MHz, CDCl₃)** δ 8.24 (dd, J = 7.7, 1.4 Hz, 1H), 8.17 (dd, J = 7.7, 1.4 Hz, 1H), 7.85 (td, J = 7.6, 1.4 Hz, 1H), 7.79 (td, J = 7.5, 1.3 Hz, 1H), 7.63 (s, 1H).

2-chloro-3-methoxynaphthalene-1,4-dione (61) Compound was obtained according to the general procedure 2 **Yield** 73% **State:** yellow solid **UPLC-MS MS** method C: Rt: 2.21(ESI)⁺: 223[M+H]⁺ **¹H-NMR (500 MHz, CDCl₃)** δ : 8.15 – 8.05 (m, 1H), 8.06 – 7.97 (m, 1H), 7.78 – 7.58 (m, 2H), 4.25 (s, 3H).

2-chloro-3-ethoxynaphthalene-1,4-dione (62) The title compound was obtained according to the general procedure 2 **Yield** 71% purity: 84% **State:** yellow solid **UPLC-MS MS** method C: Rt: 2.02 MS (ESI)⁺: 236.1-238.1[M+H]⁺ **¹H-NMR (500 MHz, CDCl₃)** δ : 8.11 – 8.04 (m, 1H), 8.06 – 7.93 (m, 1H), 7.71 – 7.63 (m, 2H), 4.56 (q, J = 7.1 Hz, 2H), 1.40 (t, J = 7.1 Hz, 3H).

2-chloro-3-propoxynaphthalene-1,4-dione (63) The title compound was obtained according to the general procedure 2 **Yield** 75% purity: 84% **State:** orange solid **UPLC-MS MS** method C: Rt: 2.39 MS (ESI)⁺: 251[M+H]⁺ **¹H-NMR (500 MHz, CDCl₃)** δ : 8.12 – 8.05 (m, 1H), 8.07 – 7.96 (m, 1H), 7.72 – 7.61 (m, 2H), 4.47 (t, J = 6.5 Hz, 2H), 1.77 (dt, J = 7.5, 6.5 Hz, 2H), 1.00 (t, J = 7.4 Hz, 3H).

2-chloro-3-isopropoxynaphthalene-1,4-dione (64) The title compound was obtained according to the general procedure 2 **Yield** 73% **State:** yellow solid **UPLC-MS MS** method C: Rt: 2.19 MS (ESI)⁺: 272[M+Na]⁺ **¹H-NMR (500 MHz, CDCl₃)** δ : 8.15 – 8.12 (m, 1H), 8.10 – 7.90 (m, 1H), 7.73 – 7.68 (m, 2H), 5.21 – 5.10 (m, 1H), 1.32 (d, J = 6.2 Hz, 6H).

2-chloro-3-phenoxy-naphthalene-1,4-dione (65) Compound was obtained according to the general procedure 2 **Yield** 62% **State:** orange solid **UPLC-MS MS** method C: Rt: 2.36 MS (ESI)⁺: 272[M+Na]⁺ **¹H-NMR (500 MHz, CDCl₃)** δ : 8.03 – 7.98 (m, 1H), 7.79 – 7.63 (m, 2H), 7.32 – 7.25 (m, 1H), 7.17 (d, J = 7.4 Hz, 2H), 7.12 – 7.06 (m, 2H), 6.99 – 6.93 (m, 1H),

2-chloro-3-(methy-lamino)naphthalene-1,4-dione (66) The title compound was obtained according to the general procedure 1 **Yield** 93% **State:** purple solid **UPLC-MS MS** method C: Rt: 1.91 MS (ESI)⁺:

222[M+Na]⁺¹H-NMR (500 MHz, CDCl₃) δ: 8.08 (dd, *J* = 7.8, 1.4, Hz, 1H), 7.96 (dd, *J* = 7.7, 1.4, Hz, 1H), 7.66 (td, *J* = 7.6, 1.4 Hz, 1H), 7.55 (td, *J* = 7.6, 1.3 Hz, 1H), 3.38 (d, *J* = 5.2 Hz, 3H).

2-chloro-3-(ethylamino)naphthalene-1,4-dione (67) The title compound was obtained according to the general procedure 1 **Yield** 95% **State**: purple solid **UPLC-MS MS** method C: Rt: 2.10 MS (ESI)⁺: 236[M+Na]⁺¹H-NMR (500 MHz, CDCl₃) δ: 8.14 – 8.04 (m, 1H), 7.96 (dd, *J* = 7.6, 1.3 Hz, 1H), 7.65 (td, *J* = 7.6, 1.3 Hz, 1H), 7.55 (td, *J* = 7.6, 1.3 Hz, 1H), 3.84 (qd, *J* = 7.2, 6.1 Hz, 2H), 1.27 (t, *J* = 7.2 Hz, 3H).

2-chloro-3-(dimethylamino) naphthalene-1,4-dione (68) The title compound was obtained according to the general procedure 1 **Yield** 85% **Purity**:92% **State**: purple solid **UPLC-MS MS** method C: Rt: 2.29 MS (ESI)⁺: 250[M+Na]⁺¹H-NMR (500 MHz, CDCl₃) δ 8.08 (dd, *J* = 7.8, 1.3 Hz, 1H), 7.97 (dd, *J* = 7.6, 1.3 Hz, 1H), 7.65 (td, *J* = 7.6, 1.3 Hz, 1H), 7.55 (td, *J* = 7.5, 1.3 Hz, 1H), 1.25 (d, *J* = 6.4 Hz, 6H).

2-chloro-3-((2-fluoro-5-(trifluoromethyl)phenyl)amino)naphthalene-1,4-dione (69) The title compound was obtained according to the general procedure 1 **Yield** 79% **Purity**:84% **State**: red solid **UPLC-MS** method C: 2.43 MS (ESI)⁺: 370[[M+H]⁺¹H-NMR (500 MHz, CDCl₃) δ: δ: 8.28-8.23 (m, 1H), 8.20 – 8.12 (m, 1H), 7.82 (td, *J* = 1.4, 7.6 Hz, 1H), 7.76 (td, *J* = 1.3, 7.5 Hz, 1H), 7.54 – 7.48 (m, 1H), 7.45 (s, 1H, NH), 7.39 (dd, *J* = 2.3, 7.3 Hz, 1H), 7.28 – 7.24 (m, 1H).¹³C-NMR (125 MHz CDCl₃), δ: 178.4, 147.6, 134.7, 134.3, 134.2, 132.5, 129.6, 127.8, 127.4, 124.8,

2-((3-(trifluoromethyl) phenyl) amino) naphthalene-1,4-dione (70) The title compound was obtained according to the general procedure 5 **Yield** 84% **State**: orange solid **UPLC-MS** method C: 2.29 MS (ESI)⁺: 318[M+H]⁺¹H-NMR (500 MHz, CDCl₃) δ: 8.07 (dd, *J* = 9.7, 7.8 Hz, 2H), 7.72 (td, *J* = 7.5, 1.3 Hz, 1H), 7.63 (td, *J* = 7.5, 1.4 Hz, 1H), 7.55 (s, 1H), 7.49 (t, *J* = 7.9 Hz, 1H), 7.42 (dd, *J* = 17.1, 8.2 Hz, 2H), 6.35 (s, 1H).

2-((4-fluoro-3-(trifluoromethyl) phenyl) amino) naphthalene-1,4-dione (71) The title compound was obtained according to the general procedure 5 **Yield** 85% **State**: orange solid **UPLC-MS** method C: 2.31 MS (ESI)⁺: 366[M+H]⁺¹H-NMR (500 MHz, CDCl₃) δ: 8.23 (dd, *J* = 7.6, 1.4 Hz, 1H), 8.16 (dd, *J* = 7.8, 1.4 Hz, 2H), 7.85 – 7.79 (m, 1H), 7.79 – 7.68 (m, 1H), 7.62 (s, 1H), 7.56 – 7.48 (m, 1H), 6.28 (s, 1H).

Synthesis of 2-(10-hydroxydecyl)-3-methylnaphthalene-1,4-dione (73)

To a solution of menadione (1 eq in acetonitrile/water 5 ml 4/1) was added 11-mono-carboxylic acids (1.5 eq) and AgNO₃ (0.3 eq). The mixture was heated to 75°C and a solution of K₂S₂O₈ (2 eq) in distilled water 3mL were added dropwise over 10 minutes, then the reaction mixture was stirred for another 90minutes. The resulting mixture was cooled, evaporated and the residue was extracted with CH₂Cl₂. The organic layer was washed with water, then dried over anhydrous Na₂SO₄ and evaporated under

reduced pressure. The crude product was purified by flash column chromatography, Biotage Isolera One system, Cartridge: ZIP KP 20g, using nHexane/EtOAc, as eluent to afford the title compound. **Yield:**30%. **State:** yellow solid **UPLC-MS** method C: 1.89 MS (ESI)+: 329[M+H]⁺**¹H-NMR (500 MHz, CDCl₃)** δ ppm 8.12-8.10 (m, 2H), 7.33-7.71 (m, 2H), 3.67 (t, J = 6.8 Hz, 2H), 2.66 (t, J = 7.4 Hz, 2H), 2.22 (s, 3H), 1.60-1.20 (m, 16H). **¹³C-NMR (125 MHz CDCl₃)**, δ ppm 181.2, 180.4, 144.4, 140.2, 135.0, 134.7, 132.8, 132.4, 126.0, 125.4, 64.3, 32.4, 29.6, 28.5, 28.0, 27.7, 24.4, 23.3, 22.5, 21.4, 14.0

Molecular modelling

The computational studies were carried out on a 1.80 GHz Intel Xeon (8 cores) processor-based system, running Ubuntu 14.04 LTS, using a Molecular Operating Environment (MOE) 2015.10 (Chemical Computing Group Inc. 2016) and Maestro v10 (Schrödinger LLC, New York, NY, 2017)

Protein preparation

All target structures were downloaded from the Protein Data Bank and completed with MAESTRO (Schrödinger v10)³⁵. In all of them, all water and co-crystallized molecules were removed, except for the ligand and FADH or HEME groups. The protein was pre-processed using the Schrödinger Protein Preparation Wizard by assigning bond orders, adding hydrogens and performing a restrained energy minimisation of the added hydrogens using the OPLS_2005 force field. Predicting protonation states of protein residues was calculated considering a temperature of 300K and a pH of 7.

Pharmacophore

For NQO1 target proteins, a pharmacophore was built with MOE 2015.10 protein-ligand interaction fingerprints (PLIF). ³⁶PLIF automatically detected the potential location features (annotation points), that constitute the pharmacophore query and binding interactions. Hydrophobic areas (Hs), aromatic rings (ARs), hydrogen bond acceptors (HBAs), aromatic rings (ARs) have been used as ligand annotation points, exclusion volumes (XVOLs) were added for binding site size definition. The prepared ligand conformations originated from a commercially available database of four different vendors (SPECS, Enamine, Life Chemicals and ChemDiv), were screened for structures that match the pharmacophore query. The molecule that matched at least three essential features of the total were saved. (Supporting information S1)

Homology modelling

The homology model was computed with the Homology Model tool of MOE 2015.10 suite. The FASTA sequence of the protein (P00156) was downloaded from the Swiss-Prot database and was modelled

on the template crystal structure (PDB:1ntz). The protein crystal structure was prepared before the homology modelling, removing water molecules and unwanted ligands. The model was verified by Structural Analysis and Verification Server (SAVES v5.0) to evaluate its stereo-chemical quality. (Supporting information S2)

Molecular Docking

All molecular docking studies were performed Maestro Glide program. Prior docking, the receptor grids were built selected the co-crystallized ligands as center and a 12 Å grid length. The ligands were prepared using the Maestro LigPrep tool by energy minimising the structures (OPLS_2005 force field), generating possible ionization states at pH 7 ± 2 , generating tautomers and low-energy ring conformers. The docking calculations were performed with standard precision, keeping the default parameters and setting 3 as number of output poses per input ligand. The docking results were visually inspected for their ability to bind the active with MOE 2015.10.

Prediction of standard reduction potential

The prediction of standard potential reduction of quinone compounds was performed using Gaussian 09.³⁷ Molecular structures were optimized at the B3LYP/6-31G(d) level of theory, and the presence of water was simulated using the Conductor-like Polarizable Continuum Model (CPCM). (Supporting information S5)

Biological assay

Cell culture

HepG2 cell line was kindly provided by Prof. Karl Hoffmann's lab, IBERS, (Aberystwyth University), while SH-SY5Y was provided Dr Emma Kidd's lab (Cardiff University). Both cell lines were cultivated under normal culture conditions (37 °C, 5% CO₂, and 90% relative humidity [rH]). All media were supplemented with antibiotics (100 units/mL penicillin, 1 µg/mL streptomycin, (Gibco), Glutamax (Gibco) as 1% of volume in a mixed solution. Fetal bovine serum (FBS, Gibco) was used as a serum at a final concentration of 10%.

Rescue of ATP level

Cellular ATP levels were quantified by CellTiter-Glo® Luminescent Cell Viability Assay (Promega). The Kit was used as recommended by the manufacturer. Briefly, the day prior to the assay cells were seeded in 96-well plates (10×10^3) in culture media (Gibco) containing 1g/L glucose supplemented with 1x penicillin/streptomycin, 1x Glutamax, 2% FBS. The day after, the media was replaced with

fresh media (without glucose and FBS) containing rotenone 10 μ M, tested compounds were added at the same time. Cells were incubated at 37°C for 2 hours, before measuring the ATP content, using the Cell Titer Glo assay. The luminescence of each well was normalized according to untreated cells (in the absence of rotenone).

Determination of cell viability assessed by CellTiter-Blue

To quantify the amount of live and dead cells, CellTiter-Blue Cell Viability Assay was used as recommended by the manufacturer. Briefly, the day prior to the assay cells were seeded in 96-well plates (10×10^3) in culture media containing 1g/l glucose supplemented with 1x penicillin/streptomycin, 1x Glutamax, 2% FBS. The day after, the media was replaced with fresh media (2% FBS, 1g/L glucose) containing 25 μ M of tested compound. Cells were incubated at 37°C for 24 hours. After 24 hours, 20 μ L of CellTiter Blue reagent was added to each well (100 μ L) and incubated for 4 h at 37 °C. Following this period, the fluorescence was measured using excitation/emission wavelengths of 560/590 nm. Data were normalized to vehicle control-treated cells.

Determination of H₂O₂ level by the ROS-Glo™ H₂O₂

The reagent ROS-Glo™ H₂O₂ (Promega) was used to quantify the level of H₂O₂ in cells, used as indicator of ROS generation. ROS-Glo™ H₂O₂ assay was carried out as instructed by the manufacturer. Briefly, cells were seeded in white 96-well plates, and the day of the assay the media was replaced with 80 μ L of a fresh media containing 25 μ M of Menadione or tested compounds, followed by 20 μ L of H₂O₂ substrate dilution buffer (containing 125 μ M of H₂O₂ substrate). The plates were incubated for 4h, and after that, 100 μ L of ROS-GLO detection solution was added to the plates. The plates were incubated at room temperature for another 20 minutes. Subsequently, the luminescence signals were measured. Mean background value from cell-free wells incubated dye was subtracted from signals

Determination of quinone reduction by WST-1

The intracellular reduction of quinones was determined using the water-soluble tetrazolium salts WST-1((2-(4-iodophenyl)-3-(4-nitrophenyl)-5-(2,4-disulfophenyl)-2H-tetrazolium (Santa Cruz Biotechnology,). The conversion of salt into the corresponding formazan dye, upon reduction by hydroquinones, was followed by reading the increase of absorbance at 450 nm using the CLARIOstar plate reader. The assay was performed as described by Tan and Berridge.²⁶

Activity and toxicity analysis in the retinal explant

Wild-type, 6–8 month old, female C57 BL/6J mice were used as the source of retinal explants. Mice were kept in a 12-h light-dark cycle with food and water available ad libitum. Maintenance and all

experimental procedures were carried out in compliance with the ARVO Statement for the Use of Animals in Ophthalmic and Vision Research and were approved by the Home Office, UK. Mice were sacrificed by cervical dislocation. Eyes were immediately enucleated, transferred to a culture dish with ice-cold HBSS (Gibco, Invitrogen Corp, Paisley, UK). The naphthoquinones activity and toxicity *ex vivo* were determined using retina explants from C57 B6 mice using the same protocol described in our previous study¹⁷. Briefly, the retina explants were placed in a 6-well plate containing compounds at various concentrations for toxicity tests, or compounds plus 100 μ M rotenone for activity tests, solubilized in 0.1% DMSO and pre-warmed Neurobasal A media. Anti-RBPMS primary antibody was used to detect RGCs cells, while Hoechst 33342 was used for nuclei stains. RBPMS positive cells and nuclei in the retinal ganglion cell layer were counted.¹⁷

The Supporting Information

Formula strings and associated biological data (CSV), complex III homology model coordinates, Virtual screening workflow, Pro-oxidant effect of naphthoquinones, NQO1 activity in the presence of a quinone, dose-response curve of idebenone, 1, 49, 58, 75, ATP rescue activity compound in SH-S5SY cell lines, DFT methods used for predicting the standard potential reduction of quinone compounds and Cartesian coordinates (\AA) of the compound 1, Metabolic stability data, copies of NMR spectra, and UPLC purity analysis for compound 52, 1, 49, 51, 58, 75, 56, 24, 53, 54, 39

AUTHOR INFORMATION

Corresponding Authors: Carmine Varricchio - School of Pharmacy and Pharmaceutical Sciences, Cardiff University, CF10 3NB, Wales, UK, Email: varricchioc@cardiff.ac.uk, orcid.org/0000-0002-1673-4768

Abbreviations Used

Structure-activity relationship (SAR), Leber's hereditary optic neuropathy (LHON), mitochondrial DNA (mtDNA), NADH dehydrogenase 4 (ND4), NADH dehydrogenase 1 (ND1), NADH dehydrogenase 6 (ND6), electron transport chain (ETC), adenosine triphosphate (ATP), retinal ganglion cells (RGCs), NAD(P)H: quinone oxidoreductase 1 (NQO1), vitamin K oxidoreductase 1 (VKORC1, vitamin K oxidoreductase 1 like 1 (VKORC1L1), flavin adenine dinucleotide (FAD), phenylalanine (Phe), reactive oxygen species (ROS), electron-donating group (EDG), electron-withdrawing group (EWG) highest occupied molecular orbital (HOMO) and lowest unoccupied molecular orbital (LUMO), polarized continuum model (PCM)

Acknowledgements

We thank the Welsh Government, Life Sciences Research Network Wales scheme and National Eye Research Centre for financial support.

Reference

- (1) Man, P. Y.; Griffiths, P. G.; Brown, D. T.; Howell, N.; Turnbull, D. M.; Chinnery, P. F. The Epidemiology of Leber Hereditary Optic Neuropathy in the North East of England. *Am.J Hum.Genet.* **2003**, *72* (2), 333–339. <https://doi.org/10.1086/346066>.
- (2) Piotrowska, A.; Korwin, M.; Bartnik, E.; Tońska, K. Leber Hereditary Optic Neuropathy - Historical Report in Comparison with the Current Knowledge. *Gene* **2015**, *555* (1), 41–49. <https://doi.org/10.1016/j.gene.2014.09.048>.
- (3) Chinnery, P. F.; Brown, D. T.; Andrews, R. M.; Singh-Kler, R.; Riordan-Eva, P.; Lindley, J.; Applegarth, D. A.; Turnbull, D. M.; Howell, N. The Mitochondrial ND6 Gene Is a Hot Spot for Mutations That Cause Leber’s Hereditary Optic Neuropathy. *Brain* **2001**, *124* (1), 209–218. <https://doi.org/10.1093/brain/124.1.209>.
- (4) Zhou, Z. J.; McCall, M. A. Retinal Ganglion Cells in Model Organisms: Development, Function and Disease. *J. Physiol.* **2008**, *586* (18), 4343–4345. <https://doi.org/10.1113/jphysiol.2008.160838>.
- (5) Nikoskelainen, E. K.; Marttila, R. J.; Huoponen, K.; Juvonen, V.; Lamminen, T.; Sonninen, P.; Savontaus, M. L. Leber’s “plus”: Neurological Abnormalities in Patients with Leber’s Hereditary Optic Neuropathy. *J. Neurol. Neurosurg. Psychiatry* **1995**, *59* (2), 160–164. <https://doi.org/10.1136/jnnp.59.2.160>.
- (6) Weissig, V. Drug Development for the Therapy of Mitochondrial Diseases. *Trends Mol. Med.* **2020**, *26* (1), 40–57. <https://doi.org/10.1016/j.molmed.2019.09.002>.
- (7) Enns, G. M. Treatment of Mitochondrial Disorders: Antioxidants and Beyond. *J. Child Neurol.* **2014**, *29* (9), 1235–1240. <https://doi.org/10.1177/0883073814538509>.
- (8) Khan, N. A.; Govindaraj, P.; Meena, A. K.; Thangaraj, K. Mitochondrial Disorders : Challenges in Diagnosis & Treatment. *Indian J Med Res* **2015**, *141* (January), 13–26.
- (9) Hospira, Z. A. N. Raxone Idebene. 44, Assessment Report (EMA/480039/2015). **2012**, *44* (June), 1–91.
- (10) Yu-Wai-Man, P.; Griffiths, P. G.; Chinnery, P. F. Mitochondrial Optic Neuropathies - Disease Mechanisms and Therapeutic Strategies. *Prog. Retin. Eye Res.* **2011**, *30* (2), 81–114.

<https://doi.org/10.1016/j.preteyeres.2010.11.002>.

- (11) Rauchová, H.; Vrbacký, M.; Bergamini, C.; Fato, R.; Lenaz, G.; Houštěk, J.; Drahot, Z. Inhibition of Glycerophosphate-Dependent H₂O₂ Generation in Brown Fat Mitochondria by Idebenone. *Biochem. Biophys. Res. Commun.* **2006**, *339* (1), 362–366.
<https://doi.org/10.1016/j.bbrc.2005.11.035>.
- (12) Angebault, C.; Gueguen, N.; Desquirit-Dumas, V.; Chevrollier, A.; Guillet, V.; Verny, C.; Cassereau, J.; Ferre, M.; Milea, D.; Amati-Bonneau, P.; Bonneau, D.; Procaccio, V.; Reynier, P.; Loiseau, D. Idebenone Increases Mitochondrial Complex i Activity in Fibroblasts from LHON Patients While Producing Contradictory Effects on Respiration. *BMC Res. Notes* **2011**, *4*, 2–7.
<https://doi.org/10.1186/1756-0500-4-557>.
- (13) Smith, T. G.; Seto, S.; Ganne, P.; Votruba, M. A Randomized, Placebo-Controlled Trial of the Benzoquinone Idebenone in a Mouse Model of OPA1-Related Dominant Optic Atrophy Reveals a Limited Therapeutic Effect on Retinal Ganglion Cell Dendropathy and Visual Function. *Neuroscience* **2016**, *319*, 92–106.
<https://doi.org/10.1016/j.neuroscience.2016.01.042>.
- (14) Seo, Y.; Park, J.; Kim, M.; Lee, H. K.; Kim, J. H.; Jeong, J. H.; Namkung, W. Inhibition of ANO1/TMEM16A Chloride Channel by Idebenone and Its Cytotoxicity to Cancer Cell Lines. *PLoS One* **2015**, *10* (7), 7–9. <https://doi.org/10.1371/journal.pone.0133656>.
- (15) Jaber, S.; Polster, B. M. Idebenone and Neuroprotection: Antioxidant, pro-Oxidant, or Electron Carrier? *J. Bioenerg. Biomembr.* **2015**, *47* (1–2), 111–118.
<https://doi.org/10.1007/s10863-014-9571-y>.
- (16) Haefeli, R. H.; Erb, M.; Gemperli, A. C.; Robay, D.; Fruh, I.; Anklin, C.; Dallmann, R.; Gueven, N. NQO1-Dependent Redox Cycling of Idebenone: Effects on Cellular Redox Potential and Energy Levels. *PLoS One* **2011**, *6* (3). <https://doi.org/10.1371/journal.pone.0017963>.
- (17) Varricchio, C.; Beirne, K.; Heard, C.; Newland, B.; Rozanowska, M.; Brancale, A.; Votruba, M. The Ying and Yang of Idebenone: Not Too Little, Not Too Much – Cell Death in NQO1 Deficient Cells and the Mouse Retina. *Free Radic. Biol. Med.* **2019**, No. November, 0–1.
<https://doi.org/10.1016/j.freeradbiomed.2019.11.030>.
- (18) Faig, M.; Bianchet, M. A.; Talalay, P.; Chen, S.; Winski, S.; Ross, D.; Amzel, L. M. Structures of Recombinant Human and Mouse NAD (P) H : Quinone Oxidoreductases : Species Comparison and Structural Changes with Substrate Binding and Release. **2000**, *97* (7).

- (19) Pidugu, L. S. M.; Mbimba, J. C. E.; Ahmad, M.; Pozharski, E.; Sausville, E. A.; Emadi, A.; Toth, E. A. A Direct Interaction between NQO1 and a Chemotherapeutic Dimeric Naphthoquinone. *BMC Struct. Biol.* **2016**, *16* (1), 1. <https://doi.org/10.1186/s12900-016-0052-x>.
- (20) Winski, S. L.; Faig, M.; Bianchet, M. A.; Siegel, D.; Swann, E.; Fung, K.; Duncan, M. W.; Moody, C. J.; Amzel, L. M.; Ross, D. Characterization of a Mechanism-Based Inhibitor of NAD(P)H:Quinone Oxidoreductase 1 by Biochemical, x-Ray Crystallographic, and Mass Spectrometric Approaches. *Biochemistry* **2001**, *40* (50), 15135–15142. <https://doi.org/10.1021/bi011324i>.
- (21) Asher, G.; Dym, O.; Tsvetkov, P.; Adler, J.; Shaul, Y. The Crystal Structure of NAD(P)H Quinone Oxidoreductase 1 in Complex with Its Potent Inhibitor Dicoumarol. *Biochemistry* **2006**, *45* (20), 6372–6378. <https://doi.org/10.1021/bi0600087>.
- (22) Crofts, A. R.; Holland, J. T.; Victoria, D.; Kolling, D. R. J.; Dikanov, S. A.; Gilbreth, R.; Lhee, S.; Kuras, R.; Kuras, M. G. The Q-Cycle Reviewed: How Well Does a Monomeric Mechanism of the Bc1 Complex Account for the Function of a Dimeric Complex? *Biochim. Biophys. Acta - Bioenerg.* **2008**, *1777* (7–8), 1001–1019. <https://doi.org/10.1016/j.bbambio.2008.04.037>.
- (23) King, M. S.; Sharpley, M. S.; Hirst, J. Reduction of Hydrophilic Ubiquinones by the Flavin in Mitochondrial NADH:Ubiquinone Oxidoreductase (Complex I) and Production of Reactive Oxygen Species. *Biochemistry* **2009**, *48* (9), 2053–2062. <https://doi.org/10.1021/bi802282h>.
- (24) Woolley, K. L.; Nadikudi, M.; Koupaei, M. N.; Corban, M.; McCartney, P.; Bissember, A. C.; Lewis, T. W.; Gueven, N.; Smith, J. A. Amide Linked Redox-Active Naphthoquinones for the Treatment of Mitochondrial Dysfunction. *Medchemcomm* **2019**, *10* (3), 399–412. <https://doi.org/10.1039/c8md00582f>.
- (25) Li, C.; Zhang, K.; Xu, X. H.; Qing, F. L. Copper-Mediated Oxidative Trifluoromethylthiolation of Quinones. *Tetrahedron Lett.* **2015**, *56* (45), 6273–6275. <https://doi.org/10.1016/j.tetlet.2015.09.117>.
- (26) Tan, A. S.; Berridge, M. V. Evidence for NAD(P)H:Quinone Oxidoreductase 1 (NQO1)-Mediated Quinone-Dependent Redox Cycling via Plasma Membrane Electron Transport: A Sensitive Cellular Assay for NQO1. *Free Radic. Biol. Med.* **2010**, *48* (3), 421–429. <https://doi.org/10.1016/j.freeradbiomed.2009.11.016>.
- (27) Dehn, D. L.; Siegel, D.; Swann, E.; Moody, C. J.; Ross, D. Biochemical, Cytotoxic, and Genotoxic Effects of ES936, a Mechanism-Based Inhibitor of NAD(P)H:Quinone Oxidoreductase 1, in

- Cellular Systems. *Mol. Pharmacol.* **2003**, 64 (3), 714–720.
<https://doi.org/10.1124/mol.64.3.714>.
- (28) von Jagow, G.; Ljungdahl, P. O.; Graf, P.; Ohnishi, T.; Trumpower, B. L. An Inhibitor of Mitochondrial Respiration Which Binds to Cytochrome b and Displaces Quinone from the Iron-Sulfur Protein of the Cytochrome Bc1 Complex. *J. Biol. Chem.* **1984**, 259 (10), 6318–6326.
- (29) Namazian, M.; Almodarresieh, H. A.; Noorbala, M. R.; Zare, H. R. DFT Calculation of Electrode Potentials for Substituted Quinones in Aqueous Solution. *Chem. Phys. Lett.* **2004**, 396 (4–6), 424–428. <https://doi.org/10.1016/j.cplett.2004.08.089>.
- (30) Méndez-hernández, D. D.; Tarakeshwar, P.; Gust, D.; Moore, T. a; Moore, A. L. Simple and Accurate Correlation of Experimental Redox Potentials and DFT-Calculated HOMO / LUMO Energies of Polycyclic Aromatic Hydrocarbons. **2013**, 2845–2848.
<https://doi.org/10.1007/s00894-012-1694-7>.
- (31) Riahi, S.; Eynollahi, S.; Ganjali, M. R. Calculation of Standard Electrode Potential and Study of Solvent Effect on Electronic Parameters of Anthraquinone-1- Carboxylic Acid. *Int. J. Electrochem. Sci.* **2009**, 4 (8), 1128–1137.
- (32) Jeon, C. J.; Strettoi, E.; Masland, R. H. The Major Cell Populations of the Mouse Retina. *J. Neurosci.* **1998**, 18 (21), 8936–8946.
- (33) Bodmer, M.; Vankan, P.; Dreier, M.; Kutz, K. W.; Drewe, J. Pharmacokinetics and Metabolism of Idebenone in Healthy Male Subjects. *Eur. J. Clin. Pharmacol.* **2009**, 65 (5), 493–501.
<https://doi.org/10.1007/s00228-008-0596-1>.
- (34) Heitz, F. D.; Erb, M.; Anklin, C.; Robay, D.; Pernet, V.; Gueven, N. Idebenone Protects against Retinal Damage and Loss of Vision in a Mouse Model of Leber’s Hereditary Optic Neuropathy. *PLoS One* **2012**, 7 (9). <https://doi.org/10.1371/journal.pone.0045182>.
- (35) Schrödinger, L. Schrödinger, LLC, New York, NY, 2018 <https://www.schrodinger.com/>. **2009**, 126.
- (36) Extensions, M. O. E.; Start-, Q. Molecular Operating Environment (MOE), 2013.08; Chemical Computing Group ULC, 1010 Sherbooke St. West, Suite #910, Montreal, QC, Canada, H3A 2R7, 2019 <http://www.chemcomp.com>. *Computing* **2010**.
- (37) Gaussian 98 (Gaussian, Inc., Pittsburgh, PA, 1998) <http://www.gaussian.com/>.